

**Non-Classical Mechanical Behavior of Elastic
Membranes of Two Independent Bending Rigidities**

By

Luxia Yu

A thesis submitted in partial fulfillment of the requirements for the degree of

Master of Science

Department of Mechanical Engineering
University of Alberta

©Luxia Yu, 2015

Abstract

The non-classical mechanical behavior of an elastic membrane of two independent bending rigidities has been studied. The major interest focuses on the case when the ratio of the Gaussian bending rigidity to the common flexural rigidity falls within the non-classical ranges which cannot be covered by a classical elastic plate with an admissible positive Poisson ratio. In this work, variational method is applied to derive the governing equation and boundary conditions for a non-classical elastic membrane characterized by two independent bending rigidities. Mechanical responses of rectangular and circular non-classical elastic membranes with different boundary conditions have been analyzed systematically and compared with those of a classical elastic plate with an admissible positive Poisson ratio under otherwise identical conditions.

For a rectangular non-classical membrane with two opposite free edges, it is shown that its deflection under a uniform transverse pressure could be considerably (even more than twice) larger than a classical elastic plate under otherwise identical conditions, while its lowest fundamental frequency and critical buckling force could be considerably (even more than 50%) lower than a classical elastic plate under otherwise identical conditions. These unexpected results suggest that, unlike classical elastic plates whose actual mechanical behavior are often not sensitive to the exact value of the admissible positive Poisson ratio, actual mechanical behavior of such a rectangular non-

classical elastic membrane is very sensitive to the ratio of the Gaussian bending rigidity to the common flexural rigidity. In particular, the overall mechanical stiffness of such a rectangular non-classical membrane could be vanishingly low when the bending rigidity ratio approaches its upper limit 0.

On the other hand, the mechanical behavior of a hinged circular non-classical elastic membrane monotonically depends on the bending rigidity ratio even in the two non-classical ranges. Actually, its overall mechanical stiffness becomes vanishingly low when the bending rigidity ratio approaches its lower limit -2, while its overall mechanical stiffness is higher than a classical elastic plate with an admissible positive Poisson ratio under otherwise identical conditions when the bending rigidity ratio goes to its upper limit 0.

For both rectangular and circular non-classical elastic membranes studied in this work, the obtained results indicate that the exact value of the Gaussian bending rigidity could be crucial, and only knowing the values of the flexural rigidity and Poisson ratio is insufficient for accurate prediction of mechanical modeling of such non-classical elastic membranes (such as biomembranes and atom-thick graphene membranes).

Preface

Chapter 2 and 3 of the thesis have been published as Luxia Yu & C.Q. Ru, “Non-classical Mechanical Behavior of an Elastic Membrane of an Independent Gaussian Bending Rigidity,” *Mathematics and Mechanics of Solids*, 2015. I was responsible for math derivation, obtaining results and writing manuscript. Dr. C.Q. Ru was the supervisory author who proposed the topic, checked the results and revised the manuscript.

Chapter 4 of the thesis is expected to be submitted for publication soon. I am responsible for math derivation, obtaining results and writing manuscript. Dr. C.Q. Ru is the supervisory author who proposed the topic, checked the results and revised the manuscript.

Acknowledgements

I would like to gratefully thank my supervisor Dr. C.Q. Ru for his encouragement and support during the two years master study. His patient guidance and assistance greatly helped me in solving technical problems and writing the thesis. He gave me lots of valuable advice to help me form a good habit and serious attitude towards research. This is the most important thing I need to learn from him. What's more, I also would like to take this opportunity to thank my supervisor Dr. C.Q. Ru for his reference letter for my Ph.D application. I heartily appreciate all his efforts in the past two years.

I also hope to say thank you to all fellow researchers in Department of Mechanical Engineering at the University of Alberta and my family and friends who help and support me all the time.

Lastly, I want to thank the financial support from NSERC during the two years.

Table of Contents

Abstract.....	ii
Preface	iv
Acknowledgements.....	v
List of Figures.....	viii
List of Tables	ix
Chapter 1 Introduction.....	1
1.1 Motivation.....	1
1.2 The objectives and outline	4
Chapter 2* Formulation of a non-classical membrane of two independent bending rigidities	6
2.1 Bending strain energy	6
2.2 Positive definiteness of the bending strain energy.....	8
2.3 Contribution of the Gaussian curvature	9
2.4 Governing equation and boundary conditions	11
Chapter 3* Mechanical behavior of a rectangular non-classical elastic membrane	15
3.1 Deflection.....	17
3.1.1 Formulation	17
3.1.2 Result and discussion	19
3.2 Vibration	22
3.2.1 Formulation	22
3.2.2 Result and discussion	24
3.3 Buckling.....	27

3.3.1 Formulation	27
3.3.2 Result and discussion	28
3.4 Conclusions	31
Chapter 4 Mechanical behavior of a circular non-classical elastic membrane	33
4.1 Deflection	34
4.1.1 Formulation	34
4.1.2 Result and discussion	35
4.2 Vibration	37
4.2.1 Formulation	37
4.2.2 Result and discussion	38
4.3 Buckling	41
4.3.1 Formulation	41
4.3.2 Result and discussion	42
4.4 Conclusions	44
Chapter 5 Conclusions and future work	47
5.1 Conclusions	47
5.2 Future work	49
Bibliography	50
Appendix A	53

List of Figures

Figure 1.1 Flat atom-thick graphene.

Figure 1.2 Biomembrane.

Figure 2.1 An elastic membrane of any arbitrary shape.

Figure 3.1 A rectangular membrane with edges ($x=0$, a) simply supported.

Figure 3.2 Transverse deflection of a rectangular non-classical membrane.

Figure 3.3 Fundamental frequency of a rectangular non-classical membrane.

Figure 3.4 Frequency of a rectangular non-classical membrane in mode (1, 2).

Figure 3.5 Critical buckling force of a rectangular non-classical membrane.

Figure 3.6 Buckling force of a rectangular non-classical membrane in mode (1, 2).

Figure 4.1 Transverse deflection of a hinged circular non-classical membrane.

Figure 4.2 Fundamental frequency of a hinged circular non-classical membrane.

Figure 4.3 Frequency of a hinged circular non-classical membrane with two nodal circles.

Figure 4.4 Critical (lowest) buckling force of a hinged circular non-classical membrane.

Figure 4.5 Buckling force of a hinged circular non-classical membrane with two nodal circles.

List of Tables

Table 1.1 Parameters of non-classical elastic membranes.

Table 3.1 Comparison of transverse deflection of a rectangular non-classical membrane
at $D_g/D=-0.7$.

Table 3.2 Comparison of frequencies of a rectangular non-classical membrane.

Table 3.3 Comparison of critical buckling force of a rectangular non-classical
membrane.

Table 4.1 Comparison of frequencies of a hinged circular non-classical membrane at
 $D_g/D=-0.7$.

Chapter 1

Introduction

1.1 Motivation

Recently, the study of the mechanical properties of graphene sheets and biomembranes has attracted vast attention due to the rapid development of the nanoelectromechanical systems. For these two dimensional “soft” sheets/plates, the bending stiffness defined as the resistance to bending is quite low but still crucial to the modeling of their bending behavior. Generally, for an elastic membrane or plate, bending strain energy density is determined by the contribution of the mean curvature and Gaussian curvature

$$\bar{U} = \frac{1}{2} D * \text{Mean Curvature} + D_g * \text{Gaussian Curvature} \quad (1.1)$$

where D is the common flexural rigidity, and D_g is the Gaussian bending rigidity.

In classical elastic plate theory, the common flexural rigidity D is defined as

$$D = \frac{Eh^3}{12(1-\nu^2)}, \quad (1.2)$$

where E is the Young's modulus of isotropic materials, ν is the Poisson ratio of a linearly isotropic elastic material, and h is the thickness. There isn't a formula like equation (1.2) to determine the (negative) Gaussian bending rigidity D_g so far. But for

isotropic and homogeneous elastic plates, the Gaussian bending rigidity D_g is related to the flexural rigidity D through the Poisson ratio ν , and the ratio is $D_g/D=(\nu-1)$.

However, for some membrane-like materials such as lipid membranes and atom-thick graphene sheets (see Figures 1.1 and 1.2), which are not a homogeneous elastic continuum layer through its thickness, the Gaussian bending rigidity and the flexural rigidity can be two independent parameters. In addition, the flexural rigidity D cannot be defined as in equation (1.2) and the actual value of the flexural rigidity D could be very much different than equation (1.2) even by a few orders of magnitude. This discrepancy stems from the fact that these membrane materials are not a continuum layer through its thickness and even the thickness is hard to be uniquely defined. Therefore, for such non-classical elastic membranes, the Gaussian bending rigidity is independent of the flexural rigidity, and the classical elastic plate relation $D_g/D=(\nu-1)$ even cannot hold approximately. Some published values of the flexural and Gaussian bending rigidities and Poisson ratio of various kinds of membranes obtained by

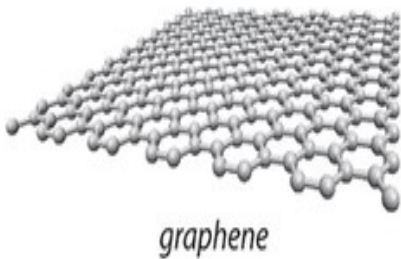


Figure 1.1 Flat atom-thick graphene.

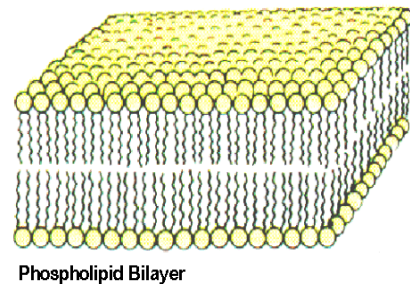


Figure 1.2 Biomembrane.

experiments or simulation are reported. The ratio D_g/D of a single-layered graphene membrane is reported to be about -0.43, where the D_g and D are $-1.12 \times 10^{-19} J$ and

$2.57 \times 10^{-19} J$, respectively (Koskinen and Kit, 2010). Wei et al. (2013) reported that the Gaussian bending rigidity of single-layered graphene membranes (about $-2.43 \times 10^{-19} J$) is independent of the flexural rigidity ($2.31 \times 10^{-19} J$) and the Poisson ratio. A range of the flexural rigidity D of the monolayer graphene is given as $1.28 \sim 2.56 \times 10^{-19} J$ and Poisson ratio is about 0.17 (Berinskii, 2014). For lipid monolayers, the ratio D_g/D is reported as -0.83 ± 0.08 , with the Gaussian bending rigidity $-0.31 \times 10^{-19} J$ (Marsh, 2006). And the Poisson ratio of lipid membranes generally falls within the range $0.39 \sim 0.54$ (Jadidi et al. 2014). Specially, the Gaussian bending rigidity of some lipid membranes is of the order $10^{-21} J$ (Deseri and Zurlo, 2013), which is two orders of magnitude higher than the flexural rigidity ($5 \times 10^{-19} J$, Harmandaris, 2006). In addition, the range $(-0.35, -0.2)$ of the ratio D_g/D has been reported for some surfactant films (Ennis, 1992). Some parameters of lipid membranes and graphene materials are listed in Table 1.1.

Table 1.1 Parameters of non-classical elastic membranes.

Material	$D_g (J)$	$D (J)$	Dg/D	ν	$\nu-1$
	-0.31×10^{-19}	-	-0.91		
Lipid membrane	-10^{-21}	5×10^{-19}	-0.002	0.54	-0.46
	-	-	-0.2		
Graphene	-1.12×10^{-19}	2.57×10^{-19}	-0.43		
	-2.43×10^{-19}	1.28×10^{-19}	-1.89	0.17	-0.83

For such non-classical elastic membranes, Helfrich (1973) developed a theoretical model for bending behavior of biomembranes of two independent bending rigidities. In

Helfrich membrane model, the positive definiteness of bending strain energy density requests the ratio of the Gaussian bending rigidity D_g to the flexural rigidity D to be within $(-2, 0)$. Obviously, the range $[-0.5, 0)$ of the ratio D_g/D , which is admissible for such non-classical Helfrich-like membranes, is inadmissible for any classical elastic plate with an admissible Poisson ratio $(-1, 0.5]$ (which corresponds to the range $(-2, -0.5]$ of the ratio D_g/D). What's more, the range $(-2, -1]$ of the ratio D_g/D corresponds to the classical elastic plate with an admissible but negative Poisson ratio, which is an unlikely case for most natural and engineering materials. To the best of our knowledge, the mechanical behavior of a Helfrich-like elastic membrane in the non-classical ranges $[-0.5, 0)$ and $(-2, -1]$ of the ratio D_g/D has not been well addressed in the existing literature. In particular, it is unclear whether setting $D_g=0$ or assuming $D_g/D=(\nu-1)$ given by the flexural rigidity and Poisson ratio could cause substantial errors.

1.2 The objectives and outline

The mechanical behavior of non-classical elastic membranes when the bending rigidity ratio D_g/D falls within the non-classical ranges has not been well studied in the existing literature. Therefore it is of great interest to investigate this significant topic. In the thesis, the major objectives are:

- 1) Derive the general governing equation and boundary conditions for Helfrich-like membranes of two independent bending rigidities;

2) Study the mechanical behavior of such non-classical elastic membranes when the bending rigidity ratio D_g/D falls within the non-classical ranges, and compare the results with that of a classical elastic plate of an admissible positive Poisson ratio.

Specifically, the thesis includes:

- 1) In Chapter 2, the governing equation and boundary conditions for such a non-classical elastic membrane of two independent bending rigidities are derived using a variational method.
- 2) In Chapter 3 and 4, the non-classical mechanical behaviors, including deflection, vibration and buckling of a rectangular membrane with two opposite free edges and a hinged circular membrane are studied, respectively.
- 3) In Chapter 5, major conclusions are summarized and future work is recommended.

Chapter 2*

Formulation of a non-classical membrane of two independent bending rigidities

In thin plate theory, two types of bending behavior are distinguished by comparing the out-of-plane deflection w to its thickness h :

- 1) Small deflection (Linear theory)-the deflection is smaller than its thickness.
- 2) Large deflection (Nonlinear theory)-the deflection is larger than or comparable to the thickness.

In the thesis, we shall only focus on the small deflection case (linear theory). Therefore, all the assumptions of the small deflection theory is still valid in the present work.

2.1 Bending strain energy

For an isotropic elastic membrane or plate, bending strain energy is determined by the contribution of mean curvature and Gaussian curvature. Specifically, it is a quadratic function of two invariants of the curvature tensor (\mathbf{C}) and characterized by the common

*This chapter is adapted from the published paper “Non-classical Mechanical Behavior of an Elastic Membrane of an Independent Gaussian Bending Rigidity,” *Mathematics and Mechanics of Solids*, 2015.

flexural rigidity (D) and the (negative) Gaussian bending rigidity (D_g).

Elastic membranes of two independent bending rigidities. For an isotropic elastic membrane of two independent bending rigidities, the Helfrich membrane model gives (Helfrich, 1973):

$$\bar{U} = \frac{1}{2} D \left[\underbrace{tr(C)}_{\text{Mean Curvature}} \right]^2 + \underline{\underline{D_g}} \underbrace{\det(C)}_{\text{Gaussian curvature}}, \quad (2.1)$$

where \bar{U} is the bending strain energy density, D and D_g are the flexural rigidity and Gaussian bending rigidity, respectively, and C is the curvature tensor given by the curvatures k_{xx} , k_{yy} , and k_{xy} :

$$C = \begin{vmatrix} k_{xx} & k_{xy} \\ k_{yx} & k_{yy} \end{vmatrix}, \quad (2.2)$$

$$k_{xx} = -\frac{\partial^2 w}{\partial x^2}, \quad k_{yy} = -\frac{\partial^2 w}{\partial y^2}, \quad k_{xy} = k_{yx} = -\frac{\partial^2 w}{\partial x \partial y}. \quad (2.3)$$

The trace ($tr(C)$) and determinant ($\det(C)$) are the two invariants of the curvature tensor C .

Classical elastic plates. For a uniform isotropic elastic plate, the bending strain energy density \bar{U} is (Timoshenko and Woinowsky-Krieger, 1959)

$$\bar{U} = \frac{1}{2} D [tr(C)]^2 + \underline{\underline{D(\nu - 1)}} \det(C). \quad (2.4)$$

where ν is the Poisson ratio within the admissible range $(-1, 0.5]$.

Comparing the bending strain energy of the classical elastic membranes/plates (see equation (2.4)) and that of a Helfrich-model (see equation (2.1)), it can be easily seen

that the common flexural rigidity D and Gaussian bending rigidity D_g are dependent for classical elastic membranes/plates, and the ratio D_g/D is given by $(\nu-1)$. But for Helfrich-like membranes, the flexural and Gaussian bending rigidities are two independent parameters, and obviously, the relation $D_g/D=\nu-1$ cannot hold for such non-classical membrane-like materials (e.g. lipid membranes and atom-thick graphene sheets) as they are not a homogeneous elastic continuum layer through its thickness. Also as shown in Table 1.1, for non-classical membranes of two independent bending rigidities, the ratio D_g/D of the Gaussian bending rigidity to the flexural rigidity can be quite different from $(\nu-1)$. Taking the single-layered graphene sheet as example, the ratio D_g/D is reported as -0.43 (Koskinen and Kit, 2010), with a Poisson ratio about 0.17 (Berinskii et al. 2014). Therefore, assuming $D_g/D=\nu-1$ could cause unacceptable errors for accurate prediction of mechanical behavior of such non-classical elastic membranes.

2.2 Positive definiteness of the bending strain energy

In the classical linear elasticity, it is well known that the positive definiteness of strain energy density requests the admissible Poisson ratio ν to be within the range $(-1, 0.5]$ and hence the bending rigidity ratio D_g/D varies from -2 to -0.5.

For Helfrich-like elastic membranes of two independent bending rigidities, the bending strain energy density is positive-definite

$$\bar{U} = \frac{D}{2} \left(\frac{\partial^2 w}{\partial x^2} + \frac{\partial^2 w}{\partial y^2} \right)^2 + D_g \left[\frac{\partial^2 w}{\partial x^2} \frac{\partial^2 w}{\partial y^2} - \left(\frac{\partial^2 w}{\partial x \partial y} \right)^2 \right] \quad , \quad (2.5)$$

$$= [k_{xx} \quad k_{yy} \quad k_{xy}] \begin{bmatrix} D & D+D_g & 0 \\ D+D_g & D & 0 \\ 0 & 0 & -2D_g \end{bmatrix} \begin{bmatrix} k_{xx} \\ k_{yy} \\ k_{xy} \end{bmatrix} > 0$$

if and only if

$$D > 0; \quad -2 < D_g / D < 0. \quad (2.6)$$

Thus the admissible range of the ratio D_g/D for such non-classical elastic membranes falls within $(-2, 0)$, containing a non-classical range $[-0.5, 0)$ of D_g/D which cannot be covered by any classical elastic plate/membrane with an admissible Poisson ratio. Furthermore, the range $(-2, -1]$ of the ratio D_g/D is inadmissible for any classical elastic plate/membrane with an admissible positive Poisson ratio. Some examples of “non-classical” elastic membranes for which the ratio D_g/D falls in the ranges $(-2, -1]$ or $[-0.5, 0)$ have been reported in the literature (see Table 1.1). Such examples include surfactant films, for which the ratio of D_g/D varies from -0.35 to 0.2 (Ennis, 1992). The mechanical behavior of such a Helfrich-like elastic membrane in the two non-classical ranges $(-2, -1]$ and $[-0.5, 0)$ of the ratio D_g/D is the major topic of the thesis.

2.3 Contribution of the Gaussian curvature

As mentioned, the bending strain energy consists of the contribution of the mean curvature and Gaussian curvature. This section will discuss the contribution of the

Gaussian curvature to the bending strain energy of non-classical Helfrich-like elastic membranes.

The bending strain energy U of non-classical elastic membranes which occupies the domain Ω of the $(x-y)$ plane is

$$U = \frac{1}{2} D \iint_{\Omega} \left(\frac{\partial^2 w}{\partial x^2} + \frac{\partial^2 w}{\partial y^2} \right)^2 dx dy + D_g \iint_{\Omega} \left[\frac{\partial^2 w}{\partial x^2} \frac{\partial^2 w}{\partial y^2} - \left(\frac{\partial^2 w}{\partial x \partial y} \right)^2 \right] dx dy. \quad (2.7)$$

Assuming the domain Ω is of an arbitrary shape, see Figure 2.1:

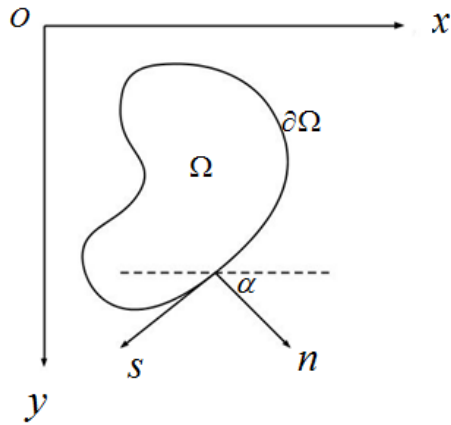


Figure 2.1 An elastic membrane of any arbitrary shape.

n and s represent the normal and tangent directions along the boundary $\partial\Omega$; α is the counter-clockwise angle between the outer normal of the boundary curve and x direction. By using the Green theorem and the transformation relations between the Cartesian and curvilinear coordinates, the Gaussian curvature term in the domain Ω (the surface integral) is converted to the line integral along the boundary $\partial\Omega$:

$$\begin{aligned}
\iint_{\Omega} \left[\frac{\partial^2 w}{\partial x^2} \frac{\partial^2 w}{\partial y^2} - \left(\frac{\partial^2 w}{\partial x \partial y} \right)^2 \right] dx dy &= \int_{\partial\Omega} \frac{\partial w}{\partial x} \frac{\partial^2 w}{\partial x \partial y} dx + \int_{\partial\Omega} \frac{\partial w}{\partial x} \frac{\partial^2 w}{\partial y^2} dy \\
&= \int_{\partial\Omega} \left(\cos \alpha \frac{\partial w}{\partial n} - \sin \alpha \frac{\partial w}{\partial s} \right) \frac{\partial}{\partial s} \left(\sin \alpha \frac{\partial w}{\partial n} + \cos \alpha \frac{\partial w}{\partial s} \right) ds
\end{aligned} \tag{2.8}$$

According to equation (2.8), we conclude that the Gaussian curvature term makes no contribution to the bending strain energy of non-classical elastic membranes in the following two cases:

- a) when the boundary is clamped ($w=0$ ($\partial w / \partial s=0$); $\partial w / \partial n=0$), the Gaussian curvature term vanishes.
- b) when the boundary is piecewise straight and hinged ($w=0$ ($\partial w / \partial s=0$); $M_n=0$), the Gaussian curvature term vanishes.

The conclusions are consistent with those of Langhaar (1952) and Zhu et al. (1989). Therefore, the Gaussian bending rigidity D_g does not affect bending behavior of the membrane when all of its edges are either clamped or straight and hinged.

2.4 Governing equation and boundary conditions

To get the general governing equation and boundary conditions for the non-classical membrane, the variational method based on the minimum potential energy (W) principle is applied.

For the given prescribed external forces, the external work V in the Cartesian coordinates is given by

$$\begin{aligned}
V = & \iint_{\Omega} q w dx dy - \iint_{\Omega} N_x^o \cdot \frac{1}{2} \left(\frac{\partial w}{\partial x} \right)^2 dx dy - \iint_{\Omega} N_y^o \cdot \frac{1}{2} \left(\frac{\partial w}{\partial y} \right)^2 dx dy - \\
& \iint_{\Omega} N_{xy}^o \cdot \frac{\partial w}{\partial x} \cdot \frac{\partial w}{\partial y} dx dy - \int_{\partial\Omega} M_n^o \frac{\partial w}{\partial n} ds + \int_{\partial\Omega} V_n^o w ds
\end{aligned} \tag{2.9}$$

where q , N_x^o , N_y^o and N_{xy}^o are the applied transverse load, in-plane tensile pre-forces and shear pre-force (per unit length) prior to bending, respectively; M_n^o is the applied bending moment per unit length and $V_n^o = Q_n^o + \partial M_{ns}^o / \partial s$ is the Kirchhoff-type effective transverse shear force, where Q_n^o and M_{ns}^o are the shear force and twisting moment per unit length.

Applying the variational method

$$\delta W = \delta U - \delta V = 0, \tag{2.10}$$

where

$$\begin{aligned}
\delta U = & D \iint (w_{,xx} \delta w_{,xx} + w_{,xx} \delta w_{,yy} + w_{,yy} \delta w_{,xx} + w_{,yy} \delta w_{,yy}) dx dy + \\
& D_g \iint (w_{,yy} \delta w_{,xx} + w_{,xx} \delta w_{,yy} - 2w_{,xy} \delta w_{,xy}) dx dy
\end{aligned} \tag{2.11}$$

and

$$\begin{aligned}
\delta V = & \iint_{\Omega} q \delta w dx dy - \int_{\partial\Omega} M_n^o \delta w_n ds + \int_{\partial\Omega} (Q_n^o + M_{ns,s}^o) \delta w ds - \iint_{\Omega} N_x^o w_{,x} \delta w_{,x} dx dy - \\
& \iint_{\Omega} N_y^o w_{,y} \delta w_{,y} dx dy - \iint_{\Omega} N_{xy}^o w_{,x} \delta w_{,y} dx dy - \iint_{\Omega} N_{xy}^o w_{,y} \delta w_{,x} dx dy
\end{aligned} \tag{2.12}$$

it can be verified that the general equation of equilibrium for static deflection of an elastic membrane of two independent bending rigidities is (for detailed derivation, see Appendix A)

$$D \nabla^4 w - q - N_x^o \frac{\partial^2 w}{\partial x^2} - N_y^o \frac{\partial^2 w}{\partial y^2} - 2N_{xy}^o \frac{\partial^2 w}{\partial x \partial y} = 0. \tag{2.13}$$

where ∇^4 is the biharmonic differential operator. In dynamic case, equation (2.13) contains an added term $\bar{m}\partial^2 w/\partial t^2$ on left-hand side, where \bar{m} is the mass density of the membrane per unit area and t is time.

Furthermore, the boundary conditions for a non-classical elastic membrane of two independent bending rigidities are given by

$$\int_{\bar{\alpha}\Omega} [D\nabla^2 w + D_g \left(\frac{\partial^2 w}{\partial x^2} \sin^2 \alpha - 2 \frac{\partial^2 w}{\partial x \partial y} \sin \alpha \cos \alpha + \frac{\partial^2 w}{\partial y^2} \cos^2 \alpha \right) + M_n^o] \frac{\partial \delta w}{\partial n} ds = 0, \quad (2.14)$$

$$\int_{\bar{\alpha}\Omega} \left[D \left[\left(\frac{\partial^3 w}{\partial x^3} + \frac{\partial^3 w}{\partial y^2 \partial x} \right) \cos \alpha + \left(\frac{\partial^3 w}{\partial y^3} + \frac{\partial^3 w}{\partial x^2 \partial y} \right) \sin \alpha \right] + D_g \frac{\partial}{\partial s} \left[\left(\frac{\partial^2 w}{\partial x^2} - \frac{\partial^2 w}{\partial y^2} \right) \sin \alpha \cos \alpha + \frac{\partial^2 w}{\partial x \partial y} (\sin^2 \alpha - \cos^2 \alpha) \right] - N_x^o \frac{\partial w}{\partial x} \cos \alpha - \left[N_y^o \frac{\partial w}{\partial y} \sin \alpha - N_{xy}^o \frac{\partial w}{\partial x} \sin \alpha - N_{xy}^o \frac{\partial w}{\partial y} \cos \alpha + Q_n^o + \frac{\partial M_{ns}^o}{\partial s} \right] \right] \delta w ds = 0 \quad . \quad (2.15)$$

In particular, as already known (equation (1.10) of Bulson, 1969), it is seen from equation (2.13) that the Gaussian bending rigidity D_g does not explicitly appear in the governing equation (2.13). For this reason, some works (Helfrich, 1973) have suggested to set $D_g=0$. However, as shown in the present thesis, actual value of the Gaussian bending rigidity D_g can play a crucial role in mechanical behavior of an elastic membrane of two independent bending rigidities through the boundary conditions.

Specifically, three typical types of boundary conditions are

$$\textit{Clamped} : w = 0; \frac{\partial w}{\partial n} = 0, \quad (2.16)$$

$$\text{Hinged : } w = 0; D\nabla^2 w + D_g \left(\frac{\partial^2 w}{\partial x^2} \sin^2 \alpha - 2 \frac{\partial^2 w}{\partial x \partial y} \sin \alpha \cos \alpha + \frac{\partial^2 w}{\partial y^2} \cos^2 \alpha \right) = 0, (2.17)$$

$$\begin{aligned} D\nabla^2 w + D_g \left(\frac{\partial^2 w}{\partial x^2} \sin^2 \alpha - 2 \frac{\partial^2 w}{\partial x \partial y} \sin \alpha \cos \alpha + \frac{\partial^2 w}{\partial y^2} \cos^2 \alpha \right) &= 0; \\ \text{Free: } D \left[\left(\frac{\partial^3 w}{\partial x^3} + \frac{\partial^3 w}{\partial y^2 \partial x} \right) \cos \alpha + \left(\frac{\partial^3 w}{\partial y^3} + \frac{\partial^3 w}{\partial x^2 \partial y} \right) \sin \alpha \right] + &. (2.18) \\ D_g \frac{\partial}{\partial s} \left[\left(\frac{\partial^2 w}{\partial x^2} - \frac{\partial^2 w}{\partial y^2} \right) \sin \alpha \cos \alpha + \frac{\partial^2 w}{\partial x \partial y} (\sin^2 \alpha - \cos^2 \alpha) \right] &= 0 \end{aligned}$$

It is noticed that the derived boundary conditions (equations (2.16-2.18)) will reduce to the known form for a classical elastic plate of arbitrary shape when $D_g/D=\nu-1$ (see for example, equation (n) on p.91 & equation (116) on p.88 of Timoshenko et al., 1959, equations (12.6) & (12.7) on p.49 of Landau and Lifshitz, 1970). What's more, it is seen from equations (2.16)-(2.18) that the Gaussian bending rigidity D_g does not appear on the boundary conditions for any clamped edge or straight hinged edge. This is in agreement with the conclusions obtained in Section 2.3 regarding the contribution of the Gaussian curvature to the bending strain energy. Hence the study on D_g -effect should focus on the case when at least part of the boundary of a non-classical elastic membrane is either free or curved and hinged. In view of its practical significance, the present work focuses on two important cases: a rectangular non-classical elastic membrane with two opposite free edges (see Chapter 3), and a circular non-classical elastic membrane with hinged edges (see Chapter 4).

Chapter 3*

Mechanical behavior of a rectangular non-classical elastic membrane

Mechanical behavior of classical elastic plates with various boundary conditions has been extensively studied in the literature (Timoshenko et al., 1959, Leissa, 1973, Kang et al., 2001, Yu, 2008), especially elastic plates of rectangular shape. Recently two dimensional membrane sheets have attracted considerable research attention. To mention a few of elastic membrane models applied to graphene sheets, for example, Atalaya et al. (2008) studied mechanical responses of clamped graphene membrane resonators in both linear and nonlinear cases using continuum elastic membrane model; Chen (2011) formulated a continuum theory for dislocation and buckling in graphene membranes. As stated, unlike classical elastic plates/membranes for which the Gaussian bending rigidity is related to the flexural rigidity by Poisson ratio, the Gaussian bending rigidity D_g of a single-layered graphene membrane is independent of the flexural rigidity and the Poisson ratio. For example, it is reported (Wei et al., 2013) that D_g of single-layered graphene membranes is about $-2.43 \times 10^{-19} J$ while the values of the flexural rigidity of single-layered graphene membranes reported in literature (Berinskii et al.,

*This chapter is adapted from the published paper “Non-classical Mechanical Behavior of an Elastic Membrane of an Independent Gaussian Bending Rigidity,” *Mathematics and Mechanics of Solids*, 2015.

2014) vary from $1.28 \sim 2.56 \times 10^{-19} J$ which gives a ratio of D_g/D ranging from -1.89 to -0.95, falling in the non-classical range (-2, -1]. Koskinen and Kit (2010) observed the ratio D_g/D of -0.43 and Ennis (1992) gave the range of ratio D_g/D of some surfactant films within (-0.35, -0.2). Therefore it is of great interest to investigate the mechanical behavior of elastic membranes of two independent bending rigidities when the bending rigidity ratio D_g/D falls outside the classical range.

For the purpose of comparison, a rectangular ($a \times b$) Helfrich-like elastic membrane whose two opposite edges parallel to the y direction are simply supported and the other two edges are free was considered with different aspect ratio ($b/a=0.5, 1, 2$), see Figure 3.1. Three important mechanical behaviors, i.e. deflection, vibration and buckling, of a rectangular non-classical membrane are studied systematically in this chapter.

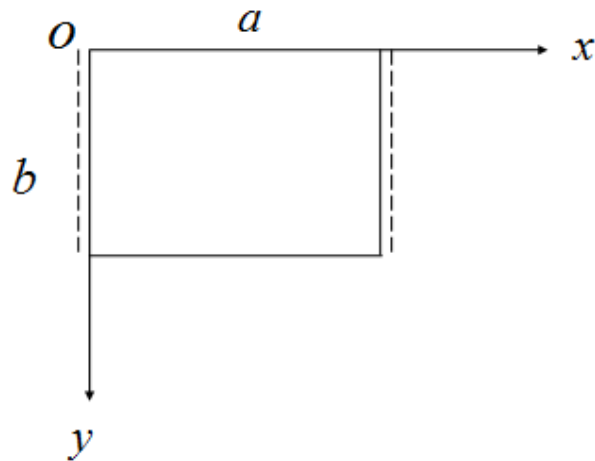


Figure 3.1 A rectangular membrane with edges ($x=0, a$) simply supported.

For a rectangular non-classical membrane with two opposite hinged edges as shown in Figure 3.1, the famous Levy method (Timoshenko et al., 1959) is applied:

$$w = \sum_{m=1}^{\infty} f_m(y) \sin\left(\frac{m\pi}{a} x\right), \quad (3.1)$$

where $f_m(y)$ are some unknown functions of y ; m is the arbitrary positive integer; and a is the length of the membrane in the x direction. The boundary conditions at $x=0, a$ are automatically satisfied. According to equation (2.18), the boundary conditions at the two free edges $y=0, b$ in Cartesian coordinates give

$$D \frac{\partial^2 w}{\partial y^2} + (D + D_g) \frac{\partial^2 w}{\partial x^2} = 0, \quad (3.2)$$

$$D \frac{\partial^3 w}{\partial y^3} + (D - D_g) \frac{\partial^3 w}{\partial x^2 \partial y} = 0. \quad (3.3)$$

It is noticed that the free-edge conditions (equations (3.2) and (3.3)) will reduce to the known form for a classical elastic plate when $D_g/D = \nu - 1$ (see equation (2.2) on p.27 and equation (2.25) on p.35 of Bulson, 1969).

3.1 Deflection

3.1.1 Formulation

Assuming the only transverse load q is constant and uniformly distributed (i.e.

$N_x^o = N_y^o = N_{xy}^o = 0$), the governing equation (2.13) reduce to

$$D \nabla^4 w = q. \quad (3.4)$$

The solution for deflection function w (equation (3.1)) which satisfies the governing equation (3.4) is of the form

$$w = \sum_{m=1}^{\infty} \left[A_m \cosh \frac{m\pi y}{a} + B_m \frac{m\pi y}{a} \sinh \frac{m\pi y}{a} + C_m \sinh \frac{m\pi y}{a} + D_m \frac{m\pi y}{a} \cosh \frac{m\pi y}{a} + \frac{2qa^4}{\pi^5 D m^5} (1 - \cos m\pi) \right] \sin \frac{m\pi x}{a}, \quad (3.5)$$

where A_m , B_m , C_m and D_m are unknowns to be determined by the edge conditions at the two free edges $y=0, b$.

Substituting equation (3.5) into boundary conditions (3.2) and (3.3) yields a system of equations:

$$[\text{Coefficient matrix}] \begin{bmatrix} A_m \\ B_m \\ C_m \\ D_m \end{bmatrix} = \begin{bmatrix} (1 + \frac{D_g}{D}) \frac{2}{\pi^5 m^5} (1 - \cos m\pi) \\ 0 \\ (1 + \frac{D_g}{D}) \frac{2}{\pi^5 m^5} (1 - \cos m\pi) \\ 0 \end{bmatrix} \frac{qa^4}{D}, \quad (3.6)$$

where the 4×4 coefficient matrix is

$$\begin{bmatrix} -\frac{D_g}{D} & 2 \\ 0 & 0 \\ -\frac{D_g}{D} \cosh \beta & 2 \cosh \beta - \frac{D_g}{D} \beta \sinh \beta \\ \frac{D_g}{D} \sinh \beta & 2 \sinh \beta + \frac{D_g}{D} \sinh \beta + \frac{D_g}{D} \beta \cosh \beta \\ 0 & 0 \\ \frac{D_g}{D} & 2 + \frac{D_g}{D} \\ -\frac{D_g}{D} \sinh \beta & 2 \sinh \beta - \frac{D_g}{D} \beta \cosh \beta \\ \frac{D_g}{D} \cosh \beta & 2 \cosh \beta + \frac{D_g}{D} \cosh \beta + \frac{D_g}{D} \beta \sinh \beta \end{bmatrix}. \quad (3.6a)$$

The unknowns A_m , B_m , C_m and D_m for each m can be determined by solving equation (3.6), and hence the deflection w is obtained in terms of the two independent bending rigidities.

3.1.2 Result and discussion

In deflection case, in order to obtain more accurate results, we take ten terms ($N=10$) of the series even though the series starts to converge well after $N=3$. Figure 3.2 presents how the dimensionless deflection wD/qa^4 at the center of the membrane with different aspect ratio varies as the ratio D_g/D changes from -2 to 0 (which is equivalent to the classical elastic plate when Poisson ratio varies within $-1 < \nu < +1$).

In all of the figures shown below including those in Chapter 4, the obtained curves are distinguished into three cases, corresponding to the three ranges of the bending rigidity ratio D_g/D :

a). D_g/D falls within $(-2, -1]$ (which is equivalent to a classical elastic plate/membrane with a negative but admissible Poisson ratio within $(-1, 0]$, an admissible but unlikely case for most natural and engineering materials);

b). D_g/D falls within $[-1, -0.5]$ (which is equivalent to a classical elastic plate/membrane with an admissible positive Poisson ratio within $[0, 0.5]$, a classical case valid for most natural and engineering materials);

c). D_g/D falls within $[-0.5, 0)$ (which is equivalent to a classical elastic plate with an inadmissible Poisson ratio in $[0.5, 1)$, a case impossible for all real isotropic linearly elastic membranes).

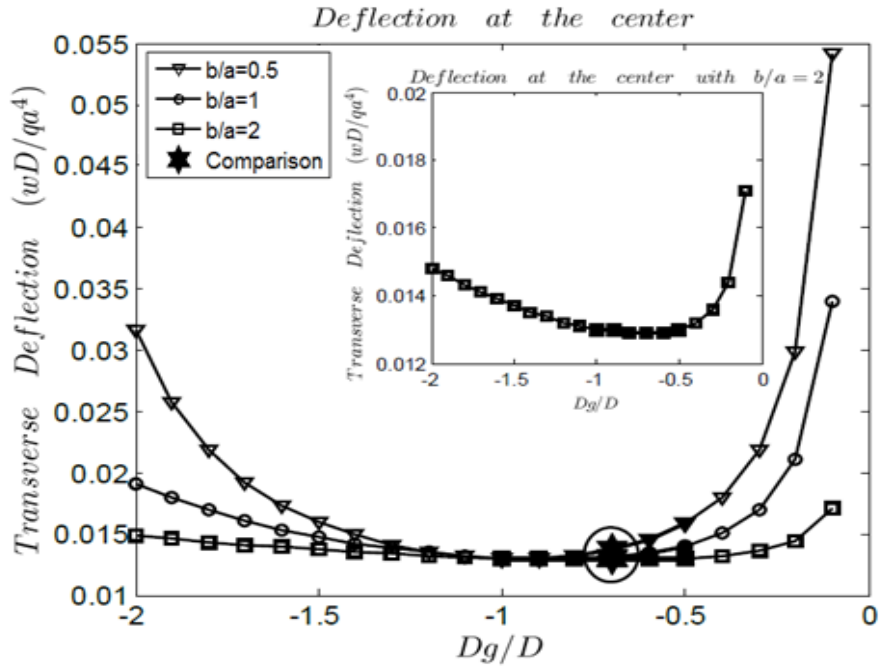


Figure 3.2 Transverse deflection of a rectangular non-classical membrane.

It is seen from Figure 3.2 that, overall speaking, the dimensionless deflection wD/qa^4 in the two cases a) and c) can be considerably (even more than twice) larger than that in case b) of a classical elastic plate of admissible positive Poisson ratio, which suggests that rectangular elastic membranes of two independent bending rigidities (such as some biomembranes or graphene sheets) could deflect considerably more than a classical elastic plate under the same transverse loading and geometrical conditions. In addition, the dimensionless deflection wD/qa^4 in the two non-classical cases a) and c) is quite sensitive to the ratio D_g/D , while wD/qa^4 is very much insensitive to the ratio D_g/D in case b) of a classical elastic plate of admissible positive Poisson ratio.

In particular, as stated before, since the Gaussian bending rigidity D_g does not explicitly appear in the governing equation (2.13), some works have suggested to set $D_g=0$.

However, as shown in Figure 3.2, the deflection of the rectangular non-classical elastic membrane studied here diverges when the Gaussian bending rigidity D_g approaches zero. Therefore, setting $D_g=0$ could cause unacceptable errors even for simpler rectangular membranes when part of its boundary is free. What's more, assuming $D_g/D=\nu-1$ for a rectangular non-classical elastic membrane could lead to inaccurate results. For example, the ratio of two independent bending rigidities of a single-layered membrane (Koskinen and Kit, 2010) has been reported to be -0.43, but the Poisson ratio of such membranes is 0.17 (Berinskii et al., 2014). The dimensionless deflection of the two different bending rigidity ratios is completely different.

Here, it's worth to mention that the deflection wD/qa^4 given in Figure 3.2 well agrees with the results shown in Timoshenko's book (1959), see Table 3.1. The symbol "star" circled in all the figures including those in Chapter 4 represents the comparisons with the existing literature.

Table 3.1 Comparison of transverse deflection of a rectangular non-classical membrane at $D_g/D=-0.7$.

—	b/a	wD/qa^4
	0.5	0.0137
This work	1	0.0131
	2	0.0129
Timoshenko	0.5	0.01377
(Table 47, $\nu=0.3$)	1	0.01309
	2	0.01289

3.2 Vibration

3.2.1 Formulation

For free vibration we have $q = N_x^o = N_y^o = N_{xy}^o = 0$. The differential equation of motion becomes

$$D\nabla^4 w + m \frac{\partial^2 w}{\partial t^2} = 0. \quad (3.7)$$

Assuming the deflection function w as

$$w = W(x, y)e^{i\omega t}, \quad (3.8)$$

where $W(x, y)$ is the mode shape function, then substituting equation (3.8) into (3.7) gives a differential equation for the mode shape function $W(x, y)$

$$\nabla^4 W - \frac{\omega^2 m}{D} W = 0. \quad (3.9)$$

The expression of $W(x, y)$ which satisfies the equation (3.9) is given by (Leissa, 1973)

$$W(x, y) = (A \cosh(\varphi y) + B \sinh(\varphi y) + C \cos(\psi y) + D \sin(\psi y)) \sin \frac{m\pi x}{a}, \quad (3.10)$$

or

$$W(x, y) = (A \cosh(\varphi y) + B \sinh(\varphi y) + C \cosh(\phi y) + D \sinh(\phi y)) \sin \frac{m\pi x}{a}, \quad (3.11)$$

where $A, B, C,$ and D are undetermined constants; φ, ψ, ϕ are defined as

$$\varphi = \sqrt{\frac{m^2 \pi^2}{a^2} + \omega \sqrt{\frac{m}{D}}}; \quad \psi = \sqrt{\omega \sqrt{\frac{m}{D}} - \frac{m^2 \pi^2}{a^2}}; \quad \phi = \sqrt{\frac{m^2 \pi^2}{a^2} - \omega \sqrt{\frac{m}{D}}}. \quad (3.12)$$

Equation (3.10) is applied when $\omega\sqrt{m/D} > m^2\pi^2/a^2$, but otherwise equation (3.11) is used. Substituting equation (3.10) or (3.11) into equations (3.2) and (3.3) for two free edges yields a system of four homogeneous linear equations for the four constants A , B , C and D :

$$[\text{Coefficient matrix}] \begin{bmatrix} A \\ B \\ C \\ D \end{bmatrix} = 0, \quad (3.13)$$

where the 4×4 coefficient matrix is

$$\begin{bmatrix} \varphi^2 - (1 + \frac{D_g}{D}) \frac{m^2 \pi^2}{a^2} & 0 \\ 0 & [\varphi^2 - (1 - \frac{D_g}{D}) \frac{m^2 \pi^2}{a^2}] \varphi \\ [\varphi^2 - (1 + \frac{D_g}{D}) \frac{m^2 \pi^2}{a^2}] \cosh \varphi b & [\varphi^2 - (1 + \frac{D_g}{D}) \frac{m^2 \pi^2}{a^2}] \sinh \varphi b \\ [\varphi^2 - (1 - \frac{D_g}{D}) \frac{m^2 \pi^2}{a^2}] \varphi \sinh \varphi b & [\varphi^2 - (1 - \frac{D_g}{D}) \frac{m^2 \pi^2}{a^2}] \varphi \cosh \varphi b \\ -[\psi^2 + (1 + \frac{D_g}{D}) \frac{m^2 \pi^2}{a^2}] & 0 \\ 0 & -[\psi^2 + (1 - \frac{D_g}{D}) \frac{m^2 \pi^2}{a^2}] \psi \\ -[\psi^2 + (1 + \frac{D_g}{D}) \frac{m^2 \pi^2}{a^2}] \cos \psi b & -[\psi^2 + (1 + \frac{D_g}{D}) \frac{m^2 \pi^2}{a^2}] \sin \psi b \\ [\psi^2 + (1 - \frac{D_g}{D}) \frac{m^2 \pi^2}{a^2}] \psi \sin \psi b & -[\psi^2 + (1 - \frac{D_g}{D}) \frac{m^2 \pi^2}{a^2}] \psi \cos \psi b \end{bmatrix} \quad (3.13a)$$

when equation (3.10) is applied, but otherwise

$$\begin{bmatrix}
\varphi^2 - (1 + \frac{D_g}{D}) \frac{m^2 \pi^2}{a^2} & 0 \\
0 & [\varphi^2 - (1 - \frac{D_g}{D}) \frac{m^2 \pi^2}{a^2}] \varphi \\
[\varphi^2 - (1 + \frac{D_g}{D}) \frac{m^2 \pi^2}{a^2}] \cosh \varphi b & [\varphi^2 - (1 + \frac{D_g}{D}) \frac{m^2 \pi^2}{a^2}] \sinh \varphi b \\
[\varphi^2 - (1 - \frac{D_g}{D}) \frac{m^2 \pi^2}{a^2}] \varphi \sinh \varphi b & [\varphi^2 - (1 - \frac{D_g}{D}) \frac{m^2 \pi^2}{a^2}] \varphi \cosh \varphi b
\end{bmatrix}$$

$$\begin{bmatrix}
\phi^2 - (1 + \frac{D_g}{D}) \frac{m^2 \pi^2}{a^2} & 0 \\
0 & [\phi^2 - (1 - \frac{D_g}{D}) \frac{m^2 \pi^2}{a^2}] \phi \\
[\phi^2 - (1 + \frac{D_g}{D}) \frac{m^2 \pi^2}{a^2}] \cosh \phi b & [\phi^2 - (1 + \frac{D_g}{D}) \frac{m^2 \pi^2}{a^2}] \sinh \phi b \\
[\phi^2 - (1 - \frac{D_g}{D}) \frac{m^2 \pi^2}{a^2}] \phi \sinh \phi b & [\phi^2 - (1 - \frac{D_g}{D}) \frac{m^2 \pi^2}{a^2}] \phi \cosh \phi b
\end{bmatrix} \cdot (3.13b)$$

The four unknowns A , B , C , and D cannot be all zero, then the determinant of the coefficient matrix must be zero, which gives a characteristic equation to determine the natural frequency for each m .

3.2.2 Result and discussion

For free vibration, the dimensionless frequency parameter $\omega a^2 \sqrt{m/D}$ with $m=1$ (which means there is only one half wave in x direction) is shown in Figures 3.3 and 3.4 for the two lowest frequencies, respectively, with two vibration modes (1, 1) and (1, 2), where the second number in the above mode codes denotes the number of half waves in y direction.

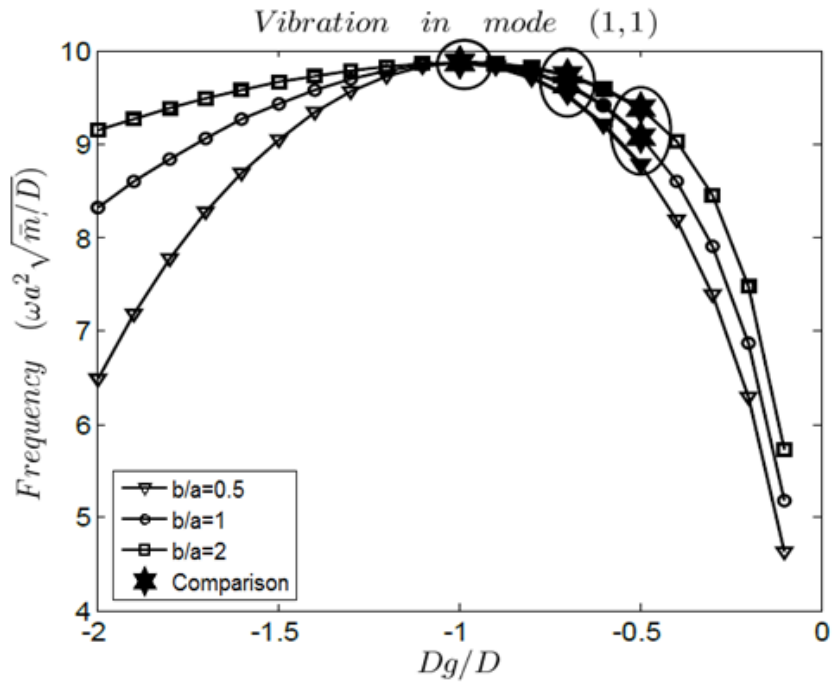


Figure 3.3 Fundamental frequency of a rectangular non-classical membrane.

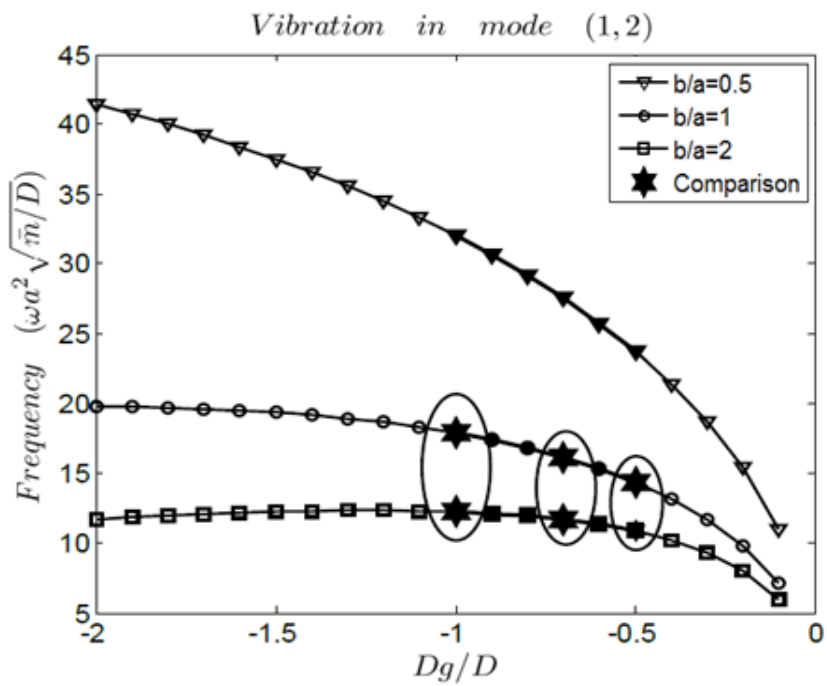


Figure 3.4 Frequency of a rectangular non-classical membrane in mode (1, 2).

Firstly, it is seen from Figure 3.3 that the dimensionless lowest fundamental frequency $\omega a^2 \sqrt{m/D}$ in the two cases a) and c) can be considerably (even more than 50%) lower than in case b) of a classical elastic plate of any real material, which suggests that rectangular elastic membranes of two independent bending rigidities could be considerably more compliant than a classical elastic plate under the same geometrical conditions. In addition, the dimensionless lowest fundamental frequency $\omega a^2 \sqrt{m/D}$ in the two cases a) and c) is quite sensitive to the ratio D_g/D , while $\omega a^2 \sqrt{m/D}$ is very much insensitive to the ratio D_g/D in case b) of a classical elastic plate of admissible positive Poisson ratio. Clearly these conclusions are consistent with those obtained in Section 3.1 for static deflection. Both suggest that the overall stiffness of rectangular elastic membranes of two independent bending rigidities could be considerably lower (even vanishing when D_g tends to zero) than a classical elastic plate of admissible positive Poisson ratio, and also is much more sensitive to the bending rigidity ratio D_g/D than a classical elastic plate of admissible positive Poisson ratio. On the other hand, it is seen from Figure 3.4 that these conclusions cannot hold for the second lowest frequency associated with the mode (1, 2).

Here, it is noticed that the results shown in Figures 3.3 and 3.4 well agree with those reported in Leissa (1973) and Kang et al. (2001), see Table 3.2.

Table 3.2 Comparison of frequencies of a rectangular non-classical membrane.

		<i>D_g/D</i>			
—	mode	<i>b/a</i>	-1	-0.7	-0.5

This work	(1,1)	0.5	9.8696	9.7362	9.3798
		1	9.8696	9.6314	9.0793
	(1,2)	0.5	12.2287	11.6845	10.8692
		1	17.8821	16.1348	14.3516
Lessia (Table 2, $\nu=0, 0.3, 0.5$)	(1,1)	1	98696	9.6314	9.0793
Kang (Table 6, 7&8, $\nu=0, 0.3, 0.5$)	(1,1)	0.5	9.870	9.736	9.380
		1	9.870	9.631	9.079
	(1,2)	0.5	12.23	11.68	10.87
		1	17.88	16.13	14.35

3.3 Buckling

3.3.1 Formulation

Considering buckling under a uniform uniaxial compressive load $N_x^0 = -P$ ($P > 0$) applied on the two simply supported edges, the buckling is governed by

$$D\nabla^4 w + P \frac{\partial^2 w}{\partial x^2} = 0. \quad (3.14)$$

Substituting the assumed deflection function w (3.1) into the governing equation (3.14) yields a characteristic equation for $f_m(y)$. Putting the solution of $f_m(y)$ back to equation (3.1), the deflection function w which satisfies the governing equation (3.14) is obtained.

Actually, the deflection function in buckling case shares the same formulas with equations (3.10) and (3.11) but with different definitions of φ, ψ, ϕ

$$\varphi = \sqrt{\frac{m\pi}{a} \left(\frac{m\pi}{a} + \sqrt{\frac{P}{D}} \right)}; \psi = \sqrt{\frac{m\pi}{a} \left(\sqrt{\frac{P}{D}} - \frac{m\pi}{a} \right)}; \phi = \sqrt{\frac{m\pi}{a} \left(\frac{m\pi}{a} - \sqrt{\frac{P}{D}} \right)}. \quad (3.15)$$

We use equation (3.10) if $\sqrt{P/D} > m\pi/a$, but otherwise equation (3.11) will be employed. Similarly, after applying the boundary conditions (equations (3.2) & (3.3)) at two free edges to equation (3.10) or (3.11), a system of four homogeneous linear equations for the four constants A, B, C and D is obtained. The formulas of coefficient matrixes ((3.13a) & (3.13b)) in free vibration case remain valid in buckling case. Under the buckling state, the unknowns A, B, C and D cannot be all zero, thus the determinant of the coefficient matrix must also be zero as the vibration case. Hence the buckling force for each m can be determined by solving the characteristic equation.

3.3.2 Result and discussion

Similar to free vibration, the dimensionless buckling force Pa^2/D with $m=1$ (which means there is only one half wave in x direction) is shown in Figures 3.5 and 3.6 for the two lowest buckling forces, respectively, with two buckling modes (1, 1) and (1, 2) where the second number in the above mode codes denotes the number of half waves in y direction.

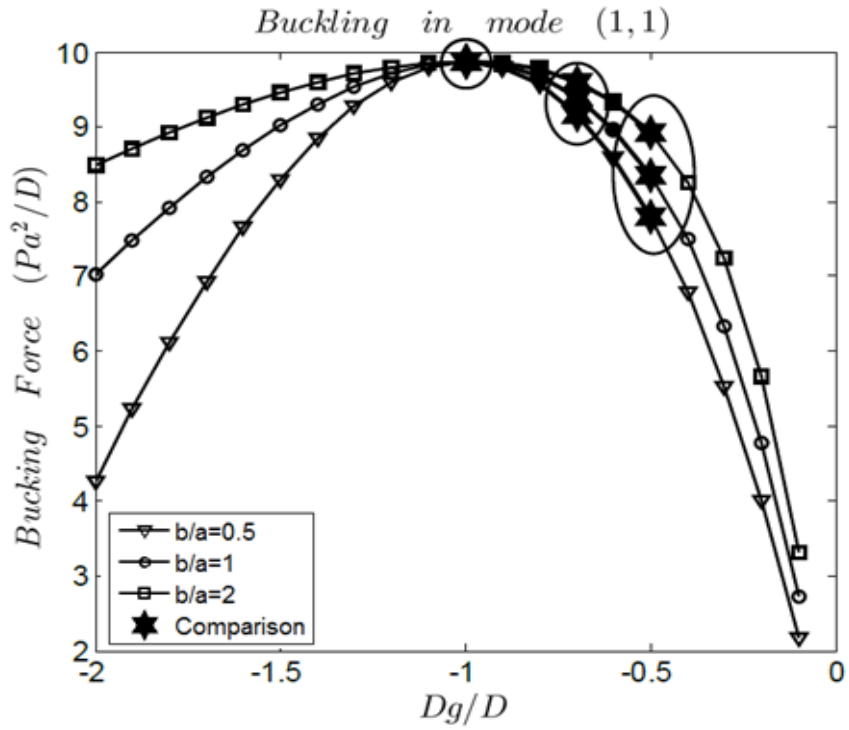


Figure 3.5 Critical buckling force of a rectangular non-classical membrane.

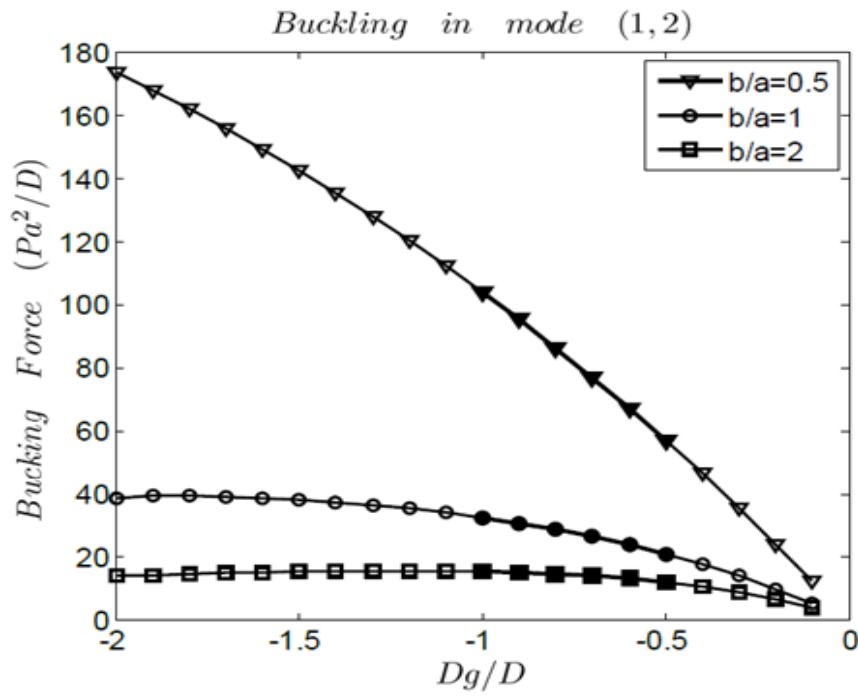


Figure 3.6 Buckling force of a rectangular non-classical membrane in mode (1, 2).

Clearly, from Figure 3.5, the dimensionless critical buckling force Pa^2/D in the two non-classical cases a) and c) can be considerably lower than in case b) of a classical elastic plate of any real material, which suggests that rectangular elastic membranes of two independent bending rigidities could be considerably more compliant than a classical elastic plate under the same geometrical conditions. In addition, the dimensionless critical buckling force Pa^2/D in the two cases a) and c) is quite sensitive to the ratio D_g/D , while it is very much insensitive to the ratio D_g/D in case b) of a classical elastic plate of admissible positive Poisson ratio.

It can be easily found that the results shown in Figure 3.5 for buckling are similar to those shown in Figure 3.3 for free vibration. Both consistently suggest that the overall stiffness of rectangular elastic membranes of two independent bending rigidities could be considerably lower than a classical elastic plate of admissible positive Poisson ratio and is much more sensitive to the bending rigidity ratio D_g/D than a classical elastic plate of admissible positive Poisson ratio. In particular, the overall mechanical stiffness of the non-classical rectangular membrane could be vanishingly low when the Gaussian bending rigidity approaches zero. Also similarly, it is seen from Figure 3.6 that these conclusions cannot hold for the second lowest buckling force associated with the buckling mode (1, 2).

Here, it is noticed that the results shown in Figure 3.5 well agree with those shown in Kang (2005) and Yu (2008), see Table 3.3. (Comparison is not available for Figure 3.6).

Table 3.3 Comparison of critical buckling force of a rectangular non-classical membrane.

—	b/a	Dg/D		
		-1	-0.7	-0.5
This work	0.5	9.8696	9.1682	9.3798
	1	9.8696	9.3989	9.0793
	2	9.869	9.6047	8.9143
Kang (Table 4, $\nu=0, 0.3, 0.5$)	0.5	9.870	9.168	9.380
	1	9.870	9.399	9.079
	2	9.868	9.605	8.915
Yu (Table 3, $\nu=0, 0.3, 0.5$)	0.5	-	-	-
	1	-	9.400	-
	2	-	9.604	-

3.4 Conclusions

Basic mechanical behavior of a rectangular elastic membrane of two independent bending rigidities is examined, with particular interest in the case when the ratio of the Gaussian bending rigidity to the common flexural rigidity falls within the non-classical ranges which cannot be covered by any classical elastic plate/membrane with an admissible positive Poisson ratio within $[0, 0.5]$. The conclusions are:

1. The overall mechanical stiffness of such a rectangular elastic non-classical membrane could be much lower than a classical elastic plate and become even

vanishingly low when the ratio of the Gaussian bending rigidity to the common flexural rigidity approaches zero.

2. The overall mechanical stiffness of such a rectangular non-classical elastic membrane is very sensitive to the ratio of the Gaussian bending rigidity D_g to the common flexural rigidity D in the non-classical ranges, although it is insensitive within the classical range $(-1, -0.5)$ covered by an elastic plate of an admissible positive Poisson ratio.

3. The present results suggested that actual value of the Gaussian bending rigidity D_g can have a crucial effect on mechanical behavior of such rectangular non-classical elastic membranes although it does not explicitly appear in the governing equation, and setting $D_g=0$ or assuming $D_g/D=\nu-1$ given by the flexural rigidity and Poisson ratio could cause unacceptable errors.

These conclusions could be helpful to explain observed scattering of the data on mechanical behavior of non-classical elastic membranes of two independent bending rigidities, such as some biomembranes and atom-thick graphene membranes.

Chapter 4

Mechanical behavior of a circular non-classical elastic membrane

In Chapter 2, we discussed the bending strain energy of non-classical elastic membranes, especially the contribution of the Gaussian curvature to the bending strain energy. As stated, the Gaussian curvature term vanishes when all edges of a plate/membrane are either clamped or piecewise straight and hinged. To study the D_g -effect on the mechanical responses of the Helfrich-like elastic membrane, our attention focuses on two practically important cases: a rectangular membrane with two opposite free edges, and a hinged circular membrane. The rectangular membrane case has been studied in Chapter 3. In this chapter, similar to the rectangular case, the deflection, vibration and buckling of a hinged circular elastic membrane will be investigated systematically with an emphasis on the non-classical ranges ((-2, -1] & [-0.5, 0)) of the ratio D_g/D .

To this end, a hinged circular membrane of radius $\rho = r$ is considered in this chapter on using the polar coordinate system (ρ, θ) . The general governing equation (2.13) and boundary conditions (equations (2.16)-(2.18)) obtained in Chapter 2 have to be transferred into the polar coordinate system. The governing equation in polar coordinates is

$$D\nabla^4 w - q - F_\rho^o \frac{\partial^2 w}{\partial \rho^2} - F_\theta^o \left(\frac{1}{\rho} \frac{\partial w}{\partial \rho} + \frac{1}{\rho^2} \frac{\partial^2 w}{\partial \theta^2} \right) - 2F_{\rho\theta}^o \frac{\partial}{\partial \rho} \left(\frac{1}{\rho} \frac{\partial w}{\partial \theta} \right) + m \frac{\partial^2 w}{\partial t^2} = 0. \quad (4.1)$$

where the biharmonic differential operator is

$$\nabla^4 = \left(\frac{\partial^2}{\partial \rho^2} + \frac{1}{\rho} \frac{\partial}{\partial \rho} + \frac{1}{\rho^2} \frac{\partial^2}{\partial \theta^2} \right)^2;$$

and q is the applied transverse load; F_ρ^o , F_θ^o and $F_{\rho\theta}^o$ are constant in-plane tensile forces and shear force. The three standard boundary conditions in polar coordinates are

$$\text{Clamped} : w = 0; \frac{\partial w}{\partial \rho} = 0, \quad (4.2)$$

$$\text{Hinged} : w = 0; D \frac{\partial^2 w}{\partial \rho^2} + (D + D_g) \frac{1}{\rho} \frac{\partial w}{\partial \rho} = 0, \quad (4.3)$$

$$\text{Free} : D \frac{\partial^2 w}{\partial \rho^2} + (D + D_g) \frac{1}{\rho} \frac{\partial w}{\partial \rho} = 0; D \frac{\partial}{\partial \rho} (\nabla^2 w) + D_g \frac{1}{\rho} \frac{\partial}{\partial \theta} \left(\frac{\partial^2 w}{\partial \rho \partial \theta} + \frac{1}{\rho} \frac{\partial w}{\partial \theta} \right) = 0. \quad (4.4)$$

It is noticed that the governing equation (4.1) is well known in many textbooks (e.g. Reddy, 1999). Also the boundary conditions (4.2-4.4) reduce to the known form of a classical circular elastic plate when $D_g/D = \nu - 1$ (equation (12.11) on p.51 of Landau and Lifshitz, 1970, equation (5.2.15a) on p.183 of Reddy, 1999).

4.1 Deflection

4.1.1 Formulation

In deflection case, similar to the rectangular membrane, only a constant transverse load q is considered. Due to the axisymmetry of the boundary conditions and the applied transverse load (i.e. the deflection w is a function of ρ), the governing differential equation becomes

$$D\left(\frac{d^2}{d\rho^2} + \frac{1}{\rho} \frac{d}{d\rho}\right)^2 w = q. \quad (4.5)$$

In this case, the general solution for deflection w which satisfies the governing equation (4.5) is

$$w = A_1 \rho^2 + A_2 + \frac{q\rho^4}{64D}, \quad (4.6)$$

where the unknown constants A_1 and A_2 can be determined by the hinged boundary conditions (4.3) at $\rho = r$. Then we obtain

$$w = \left(\frac{6 + D_g / D}{2 + D_g / D} - \frac{\rho^2}{a^2}\right) \left(1 - \frac{\rho^2}{a^2}\right) \frac{qr^4}{64D}. \quad (4.7)$$

For the purpose of comparison, the deflection of the membrane at the center is

$$w = \left(\frac{6 + D_g / D}{2 + D_g / D}\right) \frac{qr^4}{64D}. \quad (4.8)$$

4.1.2 Result and discussion

Figure 4.1 shows how the dimensionless deflection $64Dw/qr^4$ at the center of a hinged non-classical circular membrane varies as the ratio D_g/D changes from -2 to 0. The entire range of the ratio D_g/D is divided into three cases as in Chapter 3:

a). D_g/D falls within $(-2, -1]$ (which is equivalent to a classical elastic plate/membrane with a negative but admissible Poisson ratio within $(-1, 0]$, an admissible but unlikely case for most natural and engineering materials);

b). D_g/D falls within $[-1, -0.5]$ (which is equivalent to a classical elastic D_g/D falls within $[-1, -0.5]$ (which is equivalent to a classical elastic plate/membrane with an

admissible positive Poisson ratio within $[0, 0.5]$, a classical case valid for most natural and engineering materials);

c). D_g/D falls within $[-0.5, 0)$ (which is equivalent to a classical elastic plate with an inadmissible Poisson ratio in $[0.5, 1)$, a case impossible for all real isotropic linearly elastic membranes).

It is seen from Figure 4.1 that, unlike the rectangular case studied in Chapter 3, the dimensionless transverse deflection $64Dw/qr^4$ of the circular membrane monotonically depends on the ratio D_g/D in the entire range $(-2, 0)$. The dimensionless deflection in the non-classical case a) can be much (even more than a few times) larger than that of a classical elastic plate of admissible positive Poisson ratio under the same transverse loading and geometrical conditions. On the other hand, the dimensionless deflection in the non-classical case c) is slightly lower than that of a classical elastic plate. In addition,

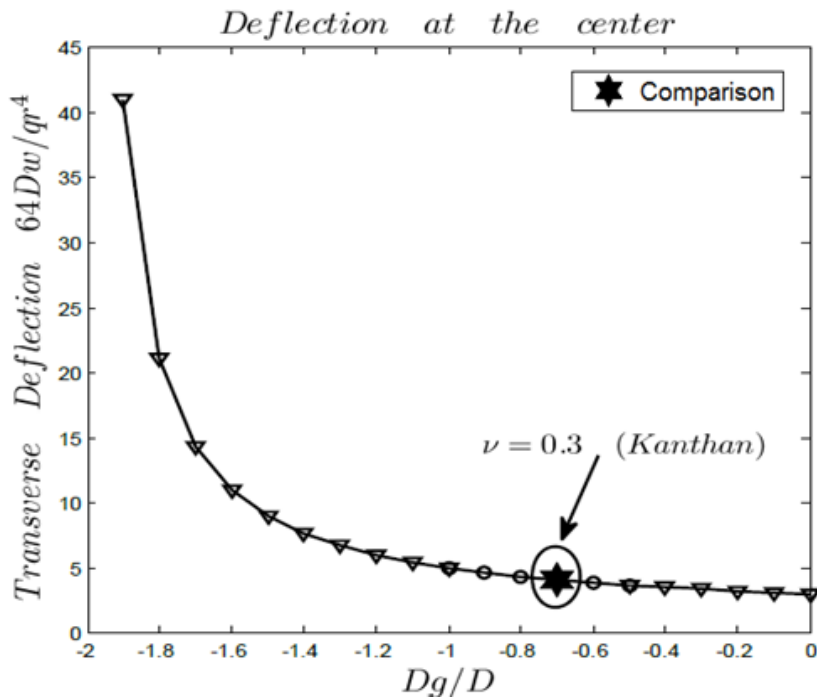


Figure 4.1 Transverse deflection of a hinged circular non-classical membrane.

the deflection of the hinged circular membrane diverges when the bending rigidity ratio D_g/D goes to the lower limit -2, while similar divergence happens for the rectangular membrane studied in Chapter 3 when the bending rigidity ratio D_g/D approaches the upper limit 0.

Here, it is worth to mention that the dimensionless deflection $64Dw/qr^4$ is 4.076 when the ratio D_g/D is -0.7, which well agrees with the value 4.07 given by (Kanthan, 1958) for a classical hinged elastic circular plate with the Poisson ratio $\nu=0.3$.

4.2 Vibration

4.2.1 Formulation

For free vibration of a hinged circular non-classical elastic membrane, the equations (3.7)-(3.9) remain valid. The mode shape function $W(\rho, \theta)$ which satisfies the governing equation and no-singularity conditions at the center ($\rho=0$) is given by (Lessia, 1969)

$$W=[B_1J_n(\gamma\rho)+B_2I_n(\gamma\rho)]\cos n\theta, \quad (4.9)$$

where $\gamma=\omega\sqrt{m/D}$; B_1, B_2 are two unknown constants to be determined by the boundary conditions (4.3) at $\rho=r$; J_n and I_n are the first kind of Bessel functions and the modified Bessel functions, respectively. The subscript n denotes the number of nodal diameters. Using equation (4.9) in boundary conditions (4.3) at $\rho=r$ gives a system of linear equations for B_1, B_2 . The unknowns B_1 and B_2 cannot be all zero, thus the determinant of the coefficient matrix must be zero:

$$\begin{vmatrix} J_n(\gamma r) & I_n(\gamma r) \\ \gamma r J_n''(\gamma r) + \left(\frac{Dg}{D} + 1\right) J_n'(\gamma r) & \gamma r J_n''(\gamma r) + \left(\frac{Dg}{D} + 1\right) J_n'(\gamma r) \end{vmatrix} = 0, \quad (4.10)$$

which yields an equation to solve for the dimensionless frequency $\omega r^2 \sqrt{m/D}$.

4.2.2 Result and discussion

For free vibration of a hinged circular non-classical membrane, the dimensionless frequency parameter $\omega r^2 \sqrt{m/D}$ with $n=0$ (which indicates that the only nodal diameter is the boundary circle) is shown in Figures 4.2 and 4.3 for two lowest frequencies, with one or two nodal circles, respectively.

Firstly, like the deflection case in Section 4.1, it is seen from Figures 4.2 and 4.3 that the

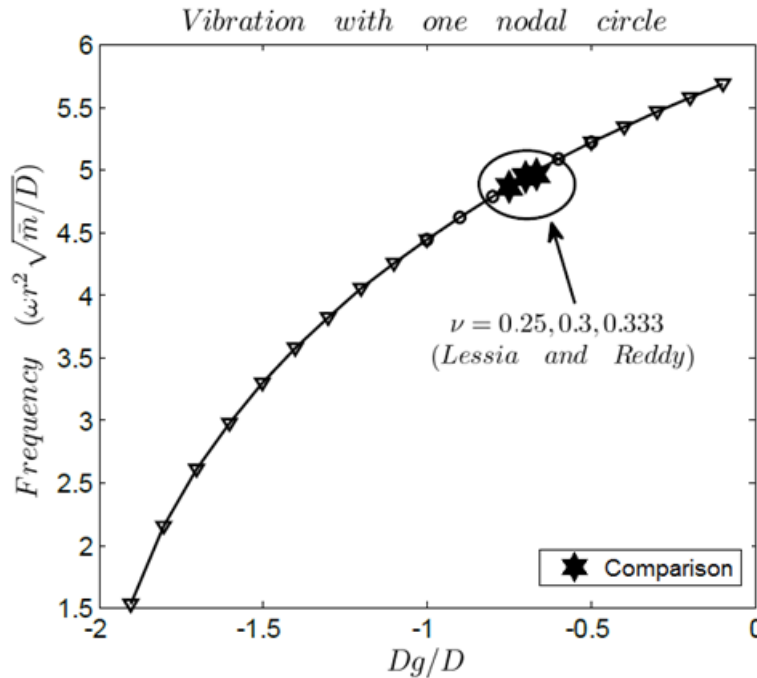


Figure 4.2 Fundamental frequency of a hinged circular non-classical membrane.

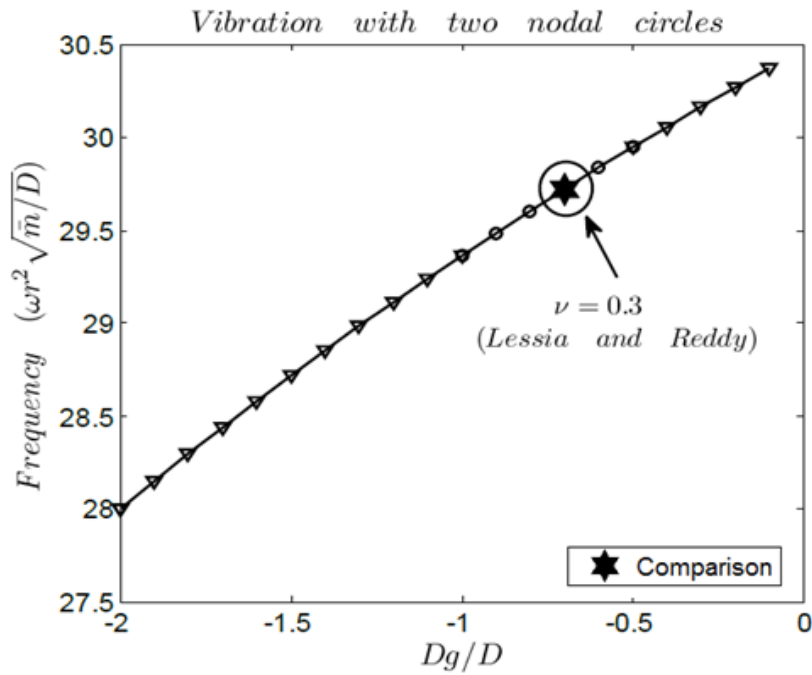


Figure 4.3 Frequency of a hinged circular non-classical membrane with two nodal circles.

dimensionless frequency $\omega r^2 \sqrt{m/D}$ monotonically depends on the ratio D_g/D . The dimensionless fundamental frequency in the non-classical case a) can be much (even a few times) lower than that of a hinged classical elastic circular plate of an admissible positive Poisson ratio under otherwise identical conditions, while the dimensionless fundamental frequency in the non-classical case c) is slightly higher than that of a hinged classical elastic circular plate. This suggests that a hinged non-classical circular elastic membrane of two independent bending rigidities could be considerably more compliant than a classical elastic plate when the bending rigidity ratio falls within (-2, -1]. In particular, it is seen from Figure 4.2 that the dimensionless fundamental frequency $\omega r^2 \sqrt{m/D}$ is vanishingly low when the bending rigidity ratio D_g/D goes to the lower

limit -2, while $\omega r^2 \sqrt{m/D}$ approaches a certain value slightly higher than that of a hinged classical elastic circular plate when the ratio D_g/D approaches the upper limit 0.

Clearly, these results are consistent with those obtained in Section 4.1 for static deflection. Both suggest that the overall stiffness of a hinged circular elastic membrane of two independent bending rigidities could be considerably lower than a classical elastic plate of admissible positive Poisson ratio when the bending rigidity ratio D_g/D falls within the range (-2, -1], while its overall mechanical stiffness could be even slightly higher than a classical elastic plate when the bending rigidity ratio D_g/D falls within the non-classical range [-0.5, 0). However, it is seen from Figure 4.3 that these conclusions do not hold for the frequency associated with two nodal circles.

Here, it is worth to mention that the dimensionless frequency $\omega r^2 \sqrt{m/D}$ shown in Figure 4.2 and 4.3 well agrees with those given in Reddy (1999) and Lessia (1969) for a hinged classical circular plate with the Poisson ratio $\nu=0.3$, see Table 4.1.

Table 4.1 Comparison of frequencies of a hinged circular non-classical membrane at $D_g/D=-0.7$.

—	Nodal circle	
	1	2
This work	4.9351	29.7200
Lessia ($\nu=0.3$)	4.977	29.76
Reddy (Table 5.5.2, $\nu=0.3$)	4.977	29.76

In addition, the values of the dimensionless fundamental frequency obtained by the present work for $D_g/D=-0.75$ and -0.667 , which are equivalent to a classical elastic plate/membrane with the Poisson ratio $\nu=0.25$ and 0.333 , respectively) are in agreement with those reported in literature (Lessia, 1969).

4.3 Buckling

4.3.1 Formulation

Now let us consider buckling of a hinged non-classical circular membrane under a uniform radial compression load $-P^*$ (per unit length, $P^*>0$) applied along the circular boundary, then $F_\rho^o=F_\theta^o = -P^*$ and the buckling is governed by

$$D\nabla^4 w - P^* \left(\frac{\partial^2 w}{\partial \rho^2} + \frac{1}{\rho} \frac{\partial w}{\partial \rho} + \frac{1}{\rho^2} \frac{\partial^2 w}{\partial \theta^2} \right) = 0. \quad (4.11)$$

The deflection function w which satisfies the governing equation (4.11) and the non-singularity conditions at the center of such a circular membrane are

$$w = [C_1 J_n(\zeta \rho) + C_2 (\zeta \rho)^n] \cos n\theta, \quad (4.12)$$

where $\zeta = \sqrt{P^* / D}$. C_1, C_2 are two unknown constants to be determined by the boundary conditions (4.3) at $\rho = r$; J_n is the first kind of Bessel functions, and n still denotes the number of nodal diameters. Substituting equation (4.12) into the boundary conditions (4.3) at $\rho = r$ gives a system of linear equations for C_1, C_2 . The unknowns C_1, C_2 cannot be all zero, thus the determinant of the coefficient matrix must be zero, which yields an equation to solve for the buckling force:

$$D\xi r J_n(\xi r) + D_g J_{n+1}(\xi r) = 0. \quad (4.13)$$

4.3.2 Result and discussion

Similar to free vibration of a hinged circular membrane, the dimensionless buckling force $r\sqrt{P^*/D}$ with $n=0$ (which indicates that the only nodal diameter is the boundary circle) is shown in Figures 4.4 and 4.5 for two buckling forces with one or two nodal circles, respectively.

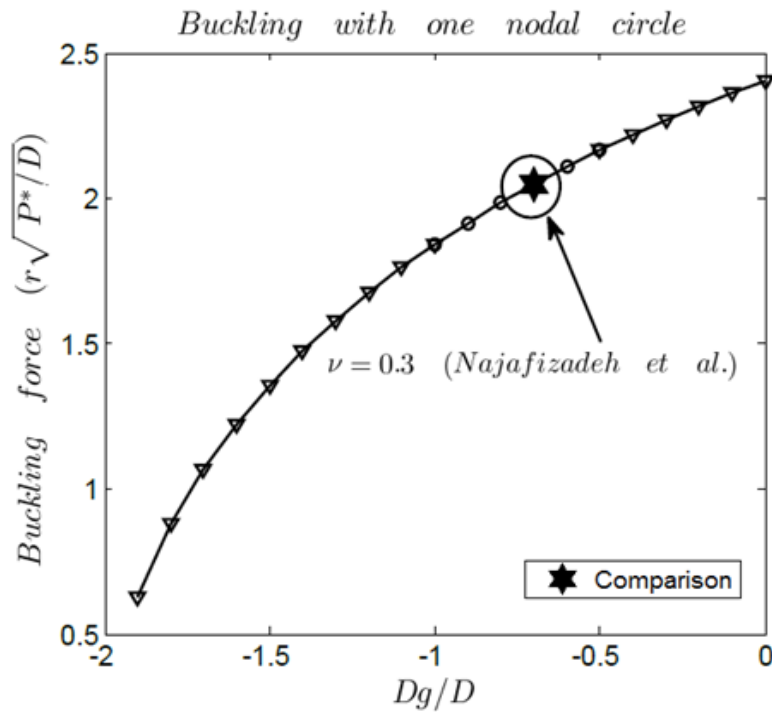


Figure 4.4 Critical (lowest) buckling force of a hinged circular non-classical membrane.

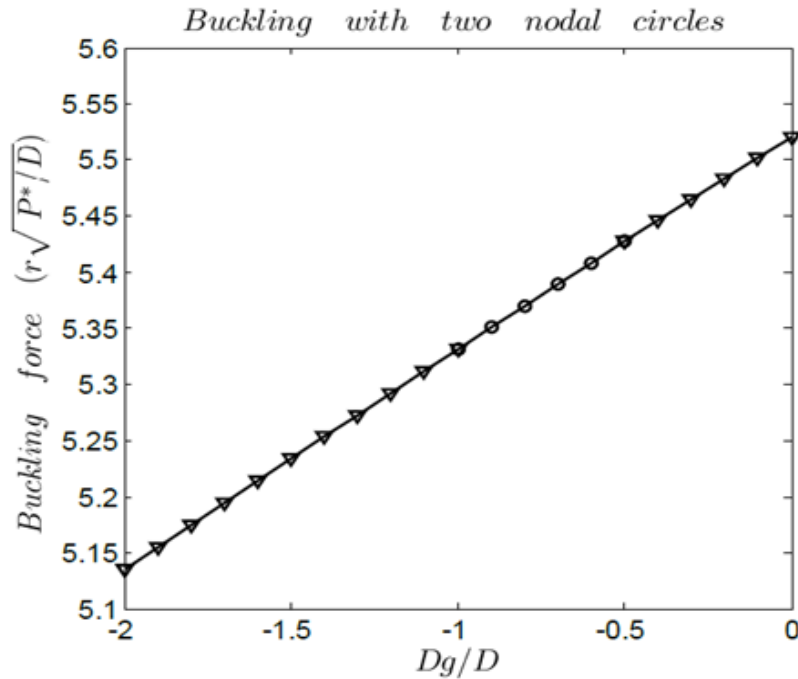


Figure 4.5 Buckling force of a hinged circular non-classical membrane with two nodal circles.

It is seen from Figure 4.4 that the dimensionless critical (lowest) buckling force $r\sqrt{P^*/D}$ monotonically depends on the ratio Dg/D . The dimensionless critical buckling force in the non-classical case a) can be much (even a few times) lower than that of a classical elastic plate of an admissible positive Poisson ratio under otherwise identical conditions, while the dimensionless critical buckling force in case c) is slightly higher than that of a classical elastic plate. Consistent with the results obtained in free vibration, this also suggests that a hinged circular elastic membrane of two independent bending rigidities could be considerably more compliant than a classical elastic plate under the same geometry conditions when the bending rigidity ratio falls within the range $(-2, -1]$.

Clearly, the results shown in Figures 4.4 and 4.5 for buckling are similar to those shown in Figures 4.2 and 4.3 for free vibration. Both consistently suggest that overall stiffness of a hinged circular elastic membrane of two independent bending rigidities could be considerably lower than a classical elastic plate of admissible positive Poisson ratio when the bending rigidity ratio falls within the range $(-2, -1]$, while its overall stiffness could be slightly higher than a classical elastic plate under otherwise identical conditions when the bending rigidity ratio falls within the range $[-0.5, 0)$.

In particular, it is seen from Figure 4.4, that the overall stiffness of a hinged circular non-classical elastic membrane could be vanishingly low when the ratio D_g/D approaches the lower limit -2 , while it approaches a certain value slightly higher than that of a hinged classical elastic circular plate when the ratio D_g/D approaches the upper limit 0 . Similarly, it is seen from Figure 4.5 that these conclusions do not hold for the buckling force associated with two nodal circles.

Here, it is noticed that the results shown in Figures 4.4 agree with some known results. For example, when the ratio $D_g/D = -0.7$, which is equivalent to a classical elastic plate/membrane with the Poisson ratio $\nu = 0.3$, the value shown in Figure 4.4 is 2.0489 , in good agreement with Najafizadeh et al. (2002) who gave a value of 2.0480 .

4.4 Conclusions

Mechanical behavior of a hinged circular elastic membrane of two independent bending rigidities is examined, with particular interest in the case when the ratio D_g/D of the

Gaussian bending rigidity to the common flexural rigidity falls within the non-classical ranges which cannot be covered by any classical elastic plate/membrane with an admissible positive Poisson ratio within $[0, 0.5]$. The main conclusions are summarized as follows:

1. The overall mechanical stiffness of a hinged circular non-classical elastic membrane monotonically depends on the ratio D_g/D of the Gaussian bending rigidity to the common flexural rigidity for the entire admissible range $(-2, 0)$ of the ratio D_g/D . The overall stiffness could be much lower than a classical elastic plate of admissible positive Poisson ratio when the ratio D_g/D falls within the range $(-2, -1]$, while it approaches a certain value slightly higher than that of a classical elastic circular plate when the ratio D_g/D approaches the upper limit 0.
2. In particular, the overall stiffness of a hinged circular non-classical elastic membrane could be vanishingly low when the ratio D_g/D approaches the lower limit -2. In this limit case, the deflection under a uniform transverse pressure becomes infinitely large, and the lowest fundamental frequency and critical buckling force become vanishingly low.
3. Based on these results and those obtained in Chapter 3 for a rectangular membrane, it is concluded that the actual effect of the Gaussian bending rigidity depends on the geometrical shape and boundary conditions of the non-classical elastic membranes, and the actual value of the Gaussian bending rigidity D_g could play an important role in mechanical behavior of such non-classical elastic membranes although it does not explicitly appear in the governing equation.

Therefore, setting $D_g=0$ or assuming $D_g/D=\nu-1$ given by the flexural rigidity and Poisson ratio could cause unacceptable substantial errors.

Chapter 5

Conclusions and future work

5.1 Conclusions

Basic mechanical behavior of a non-classical elastic membrane of two independent bending rigidities is studied, with particular interest in the cases when the ratio D_g/D of the Gaussian bending rigidity to the common flexural rigidity falls within the non-classical ranges $(-2, -1]$ and $[-0.5, 0)$ which cannot be covered by any classical elastic plate/membrane with an admissible positive Poisson ratio within $[0, 0.5]$. A rectangular membrane with two opposite free edges and a hinged circular membrane are examined systematically. The major conclusions are summarized below:

1. For a rectangular non-classical elastic membrane of two independent bending rigidities, its mechanical behavior is a non-monotonic function of the ratio D_g/D . The results indicated that the overall mechanical stiffness of such a rectangular elastic membrane in the non-classical ranges of the ratio D_g/D is much lower than that of a classical elastic plate/membrane with an admissible positive Poisson ratio under otherwise identical conditions. In addition, the overall mechanical stiffness of such rectangular membranes in the non-classical ranges is much more sensitive to the ratio D_g/D than a classical elastic plate of an admissible positive Poisson ratio.

2. On the other hand, the mechanical behavior of a hinged circular non-classical membrane monotonically depends on the ratio D_g/D even in the two non-classical ranges, and its overall stiffness increases monotonically as the ratio D_g/D increases from -2 to 0 in the entire admissible range of D_g/D . Specifically, the overall stiffness of a hinged circular non-classical elastic membrane in non-classical range (-2, -1] could be much lower than a classical elastic plate of admissible positive Poisson ratio, while the overall stiffness in non-classical range [-0.5, 0) is higher than a classical elastic plate of admissible positive Poisson ratio under otherwise identical conditions.

3. In particular, the overall mechanical stiffness of a rectangular non-classical membrane with two opposite free edges could be vanishingly low when the ratio D_g/D approaches its upper limit $D_g/D=0$, while the overall mechanical stiffness of a hinged circular non-classical membrane could be vanishingly low when the ratio D_g/D approaches its lower limit $D_g/D=-2$.

4. For both cases, the present results suggested that the actual effect of the Gaussian bending rigidity depends on the geometrical shape and boundary conditions of the non-classical elastic membranes, and the actual value of the Gaussian bending rigidity D_g plays a crucial role in mechanical behavior of such non-classical elastic membranes although it does not explicitly appear in the governing equation. Therefore setting D_g to be zero or assuming $D_g/D=\nu-1$ given by the flexural rigidity and Poisson ratio could cause unacceptable substantial errors.

The general governing equation and boundary conditions of non-classical membrane of two independent bending rigidities derived in the present work can be used for the future study of mechanical behavior of such non-classical elastic membranes, like some biomembranes and atom-thick graphene monolayers. And some results obtained in the present thesis could provide plausible explanation and useful insight for some mechanical behavior of such non-classical elastic membranes reported in the literature.

5.2 Future work

In the thesis, we only deal with the small deflection problems of non-classical elastic membranes of two independent bending rigidities. A major topic for future work is the large deflection bending behavior of such non-classical elastic membranes of two independent bending rigidities. In that case, the governing equations would be nonlinear and the effect of the Gaussian bending rigidity on mechanical behavior is expected to be quite different than the linear small deflection case studied in the present thesis.

Bibliography

Atalaya, J, Isacson, A, and Kinaret, JM. Continuum elastic modeling of graphene resonators. *Nano Lett.* 2008; 8(12): 4196-4200.

Berinskii, IE, Krivtsov, AM, and Kudarova, AM. Bending stiffness of graphene sheet. *Phys. Mesomech.* 2014; 17(4): 356-364.

Bulson, PS. *The Stability of Flat Plates*. New York: American Elsevier, 1969.

Chen, S, and Chrzan, DC. Continuum theory of dislocation and buckling in graphene. *Phys. Rev. B* 2011; 84: 214103.

Deseri L, and Zurlo G. The stretching elasticity of biomembranes determines their line tension and bending rigidity. *Biomech. Model. Mechanobiol.* 2013; 12: 1233-1242.

Ennis, J. Spontaneous curvature of surfactant films. *J. Chem. Phys.* 1992; 97(1): 663-678.

Harmandaris, VA, and Deserno, M. A novel method for measuring the bending rigidity of model lipid membranes by simulating tethers. *J. Chem. Phys.* 2006; 125: 204905.

Helfrich, W. Elastic properties of lipid bilayers: Theory and possible experiments. *Z. Naturforsch.* 1973; 28C: 693-703.

Jadidi, T, Seyyed-Allaei, H, Tabar, MRR, and Mashaghi, A. Poisson's ratio and Young's modulus of lipid bilayers in different phases. *Front. Bioeng. Biotechnol.* 2014; 2: 8.

Kang, JH, and Leissa, AW. Vibration and buckling of SS-F-SS-F rectangular plates loaded by in-plane moments. *Int. J. Struct. Stab. Dy.* 2001; 1(4): 527-543.

Kang, JH, and Leissa, AW. Exact solution for the buckling of rectangular plates having linearly varying in-plane loading on two opposite simply supported edges. *Int. J. Solids. Struct.* 2005; 42: 4220-4238.

Kanthan, CL. Bending and vibration of elastically restrained circular plates. *J. Franklin Inst.* 1958; 265(6): 483-491.

Koskinen, P, and Kit, OO. Approximate modeling of spherical membranes. *Phys. Rev. B.* 2010; 82: 235420.

Landau, LD, and Lifshitz, EM. *Theory of Elasticity*. Oxford: Pergamon Press, 1970.

Langhaar, HL. Note on the energy of bending of plates, *J. App. Mech.* 1952; 19(2): 228.

Leissa, AW. The free vibration of rectangular plates. *J. Sound Vib.* 1973; 31(3): 257-293.

Leissa, AW. *Vibration of plates*. Washington: U. S. Government Printing, 1969.

Marsh, D. Elastic Curvature constants of lipid monolayers and bilayers. *Chem. Phys. Lipids* 2006; 144: 146-159.

Najafizadeh, MM, and Eslami, MR. Buckling analysis of circular plates of functionally graded materials under uniform radial compression. *Int. J. Mech. Sci.* 2002; 44: 2479-2493.

Reddy, JN. *Theory and Analysis of Elastic Plates*. Philadelphia: Taylor & Francis, 1999.

Timoshenko, S, and Woinowsky-Krieger, S. *Theory of Plates and Shells*. New York: McGraw-Hill, 1959.

Wei, Y, Wang, B, Wu, J, Yang, R, and Dunn, ML. Bending rigidity and Gaussian bending stiffness of single-layered graphene. *Nano Lett.* 2013; 13: 26-30.

Yu, LH. Buckling of rectangular plates on an elastic foundation using the levy method. *AIAA Journal* 2008; 46(12): 3163-3166.

Zhu, C, and Dimaggio, FL. Contribution of Gaussian curvature to strain energy of plates. *J. Eng. Mech.* 1989; 115: 1434-1440.

Appendix A

The detailed derivation of the governing equation (2.13) and boundary conditions (2.16-2.18) given in Chapter 2 are summarized in the Appendix A.

The variational formulation of the bending strain energy is

$$\begin{aligned} \delta U = D \iint (w_{,xx} \delta w_{,xx} + w_{,xx} \delta w_{,yy} + w_{,yy} \delta w_{,xx} + w_{,yy} \delta w_{,yy}) dx dy + \\ D_g \iint (w_{,yy} \delta w_{,xx} + w_{,xx} \delta w_{,yy} - 2w_{,xy} \delta w_{,xy}) dx dy \end{aligned} \quad , \quad (\text{A.1})$$

and the external work is

$$\begin{aligned} \delta V = \iint_{\Omega} q \delta w dx dy - \int_{\partial\Omega} M_n^o \delta w_{,n} ds + \int_{\partial\Omega} (Q_n^o + M_{ns,s}^o) \delta w ds - \iint_{\Omega} N_x^o w_{,x} \delta w_{,x} dx dy - \\ \iint_{\Omega} N_y^o w_{,y} \delta w_{,y} dx dy - \iint_{\Omega} N_{xy}^o w_{,x} \delta w_{,y} dx dy - \iint_{\Omega} N_{xy}^o w_{,y} \delta w_{,x} dx dy \end{aligned} \quad . \quad (\text{A.2})$$

The first term of (A.1) is

$$\begin{aligned} \iint_{\Omega} w_{,xx} \delta w_{,xx} dx dy &= \iint_{\Omega} \left[\frac{\partial}{\partial x} \left(\frac{\partial^2 w}{\partial x^2} \frac{\partial \delta w}{\partial x} \right) - \frac{\partial^3 w}{\partial x^3} \frac{\partial \delta w}{\partial x} \right] dx dy \\ &= \iint_{\Omega} \left[\frac{\partial}{\partial x} \left(\frac{\partial^2 w}{\partial x^2} \frac{\partial \delta w}{\partial x} \right) - \frac{\partial}{\partial x} \left(\frac{\partial^3 w}{\partial x^3} \delta w \right) + \frac{\partial^4 w}{\partial x^4} \delta w \right] dx dy \quad . \quad (\text{A.3}) \\ &= \iint_{\Omega} \frac{\partial^4 w}{\partial x^4} \delta w dx dy + \int_{\partial\Omega} \left(\frac{\partial^2 w}{\partial x^2} \frac{\partial \delta w}{\partial x} - \frac{\partial^3 w}{\partial x^3} \delta w \right) dy \end{aligned}$$

The transformation relations are

$$\begin{aligned}
\frac{\partial}{\partial n} &= \cos \alpha \frac{\partial}{\partial x} + \sin \alpha \frac{\partial}{\partial y} \\
\frac{\partial}{\partial s} &= -\sin \alpha \frac{\partial}{\partial x} + \cos \alpha \frac{\partial}{\partial y} \\
\frac{\partial}{\partial x} &= \cos \alpha \frac{\partial}{\partial n} - \sin \alpha \frac{\partial}{\partial s} \\
\frac{\partial}{\partial y} &= \sin \alpha \frac{\partial}{\partial n} + \cos \alpha \frac{\partial}{\partial s} \\
dy &= \cos \alpha ds; \quad -dx = \sin \alpha ds
\end{aligned} \tag{A.4}$$

Apply (A.4) into (A.3) and integrate by parts, we have

$$\begin{aligned}
(A.3) &= \iint_{\Omega} \frac{\partial^4 w}{\partial x^4} \delta w dx dy + \int_{\partial\Omega} \frac{\partial^2 w}{\partial x^2} \left(\frac{\partial \delta w}{\partial n} \cos \alpha - \frac{\partial \delta w}{\partial s} \sin \alpha \right) \cos \alpha ds - \int_{\partial\Omega} \frac{\partial^3 w}{\partial x^3} \delta w \cos \alpha ds \\
&= \iint_{\Omega} \frac{\partial^4 w}{\partial x^4} \delta w dx dy - \left[\underbrace{\left(\frac{\partial^2 w}{\partial x^2} \sin \alpha \cos \alpha \delta w \right)_s}_{\text{marked in (A.5)}} - \int_{\partial\Omega} \frac{\partial}{\partial s} \left(\frac{\partial^2 w}{\partial x^2} \sin \alpha \cos \alpha \right) \delta w ds \right] \\
&\quad - \int_{\partial\Omega} \frac{\partial^3 w}{\partial x^3} \delta w \cos \alpha ds + \int_{\partial\Omega} \frac{\partial^2 w}{\partial x^2} \frac{\partial \delta w}{\partial n} \cos^2 \alpha ds \\
&= \iint_{\Omega} \frac{\partial^4 w}{\partial x^4} \delta w dx dy + \int_{\partial\Omega} \frac{\partial^2 w}{\partial x^2} \frac{\partial \delta w}{\partial n} \cos^2 \alpha ds + \int_{\partial\Omega} \frac{\partial}{\partial s} \left(\frac{\partial^2 w}{\partial x^2} \sin \alpha \cos \alpha \right) \delta w ds \\
&\quad - \int_{\partial\Omega} \frac{\partial^3 w}{\partial x^3} \delta w \cos \alpha ds
\end{aligned} \tag{A.5}$$

the term marked in (A.5) is zero since the boundary curve is closed. Similarly,

$$\begin{aligned}
\iint_{\Omega} w_{,xx} \delta w_{,yy} dx dy &= \iint_{\Omega} \frac{\partial^4 w}{\partial x^2 \partial y^2} \delta w dx dy + \int_{\partial\Omega} \left[\frac{\partial^3 w}{\partial x^2 \partial y} - \frac{\partial^2 w}{\partial x^2} \frac{\partial \delta w}{\partial y} \right] dx \\
&= \iint_{\Omega} \frac{\partial^4 w}{\partial x^2 \partial y^2} \delta w dx dy + \int_{\partial\Omega} \frac{\partial^2 w}{\partial x^2} \frac{\partial \delta w}{\partial n} \sin^2 \alpha ds \\
&\quad - \int_{\partial\Omega} \frac{\partial}{\partial s} \left(\frac{\partial^2 w}{\partial x^2} \sin \alpha \cos \alpha \right) \delta w ds - \int_{\partial\Omega} \frac{\partial^3 w}{\partial x^2 \partial y} \delta w \sin \alpha ds ; \tag{A.6}
\end{aligned}$$

$$\begin{aligned} \iint_{\Omega} w_{,yy} \delta w_{,xx} dx dy &= \iint_{\Omega} \frac{\partial^4 w}{\partial x^2 \partial y^2} \delta w dx dy + \int_{\partial\Omega} \frac{\partial^2 w}{\partial y^2} \frac{\partial \delta w}{\partial n} \cos^2 \alpha ds \\ &\quad + \int_{\partial\Omega} \frac{\partial}{\partial s} \left(\frac{\partial^2 w}{\partial y^2} \sin \alpha \cos \alpha \right) \delta w ds - \int_{\partial\Omega} \frac{\partial^3 w}{\partial x \partial y^2} \cos \alpha \delta w ds \end{aligned} \quad ; \quad (\text{A.7})$$

$$\begin{aligned} \iint_{\Omega} w_{,yy} \delta w_{,yy} dx dy &= \iint_{\Omega} \frac{\partial^4 w}{\partial y^4} \delta w dx dy + \int_{\partial\Omega} \frac{\partial^2 w}{\partial y^2} \frac{\partial \delta w}{\partial n} \sin^2 \alpha ds \\ &\quad - \int_{\partial\Omega} \frac{\partial}{\partial s} \left(\frac{\partial^2 w}{\partial y^2} \sin \alpha \cos \alpha \right) \delta w ds + \int_{\partial\Omega} \frac{\partial^3 w}{\partial y^3} \delta w \sin \alpha ds \end{aligned} \quad ; \quad (\text{A.8})$$

$$\begin{aligned} \iint_{\Omega} 2w_{,xy} \delta w_{,xy} dx dy &= 2 \iint_{\Omega} \frac{\partial^4 w}{\partial x^2 \partial y^2} \delta w dx dy + 2 \int_{\partial\Omega} \frac{\partial^2 w}{\partial x \partial y} \frac{\partial \delta w}{\partial n} \sin \alpha \cos \alpha ds \\ &\quad + \int_{\partial\Omega} \frac{\partial}{\partial s} \left[\frac{\partial^2 w}{\partial x \partial y} (\sin^2 \alpha - \cos^2 \alpha) \right] \delta w ds \quad ; \quad (\text{A.9}) \\ &\quad - \int_{\partial\Omega} \frac{\partial^3 w}{\partial x \partial y^2} \delta w \cos \alpha ds - \int_{\partial\Omega} \frac{\partial^3 w}{\partial y \partial x^2} \delta w \sin \alpha ds \end{aligned}$$

The terms related to the in-plane forces in (A.2) give

$$\begin{aligned} \iint_{\Omega} N_x^o w_{,x} \delta w_{,x} dx dy &= \iint_{\Omega} N_x^o \left[\frac{\partial}{\partial x} \left(\frac{\partial w}{\partial x} \delta w \right) - \frac{\partial^2 w}{\partial x^2} \delta w \right] dx dy \\ &= \int_{\partial\Omega} N_x^o \frac{\partial w}{\partial x} \delta w dy - \iint_{\Omega} N_x^o \frac{\partial^2 w}{\partial x^2} \delta w dx dy \quad ; \quad (\text{A.10}) \\ &= \int_{\partial\Omega} N_x^o \frac{\partial w}{\partial x} \delta w \cos \alpha ds - \int_{\partial\Omega} N_x^o \frac{\partial w}{\partial x} \delta w dy \end{aligned}$$

$$\begin{aligned} \iint_{\Omega} N_y^o w_{,y} \delta w_{,y} dx dy &= \iint_{\Omega} N_y^o \left[\frac{\partial}{\partial y} \left(\frac{\partial w}{\partial y} \delta w \right) - \frac{\partial^2 w}{\partial y^2} \delta w \right] dx dy \\ &= - \int_{\partial\Omega} N_y^o \frac{\partial w}{\partial y} \delta w dx - \iint_{\Omega} N_y^o \frac{\partial^2 w}{\partial y^2} \delta w dx dy \quad ; \quad (\text{A.11}) \\ &= \int_{\partial\Omega} N_y^o \frac{\partial w}{\partial y} \delta w \sin \alpha ds - \iint_{\Omega} N_y^o \frac{\partial^2 w}{\partial y^2} \delta w dx dy \end{aligned}$$

$$\begin{aligned}
\iint_{\Omega} N_{xy}^o w_{,x} \delta w_{,y} dx dy &= \iint_{\Omega} N_{xy}^o \left[\frac{\partial}{\partial y} \left(\frac{\partial w}{\partial x} \delta w \right) - \frac{\partial^2 w}{\partial x \partial y} \delta w \right] dx dy \\
&= - \int_{\partial\Omega} N_{xy}^o \frac{\partial w}{\partial x} \delta w dx - \iint_{\Omega} N_{xy}^o \frac{\partial^2 w}{\partial x \partial y} \delta w dx dy \quad ; \quad (A.12) \\
&= \int_{\partial\Omega} N_{xy}^o \frac{\partial w}{\partial x} \delta w \sin \alpha ds - \iint_{\Omega} N_{xy}^o \frac{\partial^2 w}{\partial x \partial y} \delta w dx dy
\end{aligned}$$

$$\begin{aligned}
\iint_{\Omega} N_{xy}^o w_{,y} \delta w_{,x} dx dy &= \iint_{\Omega} N_{xy}^o \left[\frac{\partial}{\partial x} \left(\frac{\partial w}{\partial y} \delta w \right) - \frac{\partial^2 w}{\partial x \partial y} \delta w \right] dx dy \\
&= \int_{\partial\Omega} N_{xy}^o \frac{\partial w}{\partial y} \delta w dy - \iint_{\Omega} N_{xy}^o \frac{\partial^2 w}{\partial x \partial y} \delta w dx dy \quad . \quad (A.13) \\
&= \int_{\partial\Omega} N_{xy}^o \frac{\partial w}{\partial y} \delta w \cos \alpha ds - \iint_{\Omega} N_{xy}^o \frac{\partial^2 w}{\partial x \partial y} \delta w dx dy
\end{aligned}$$

Substitute the equations (A.5)~(A.12) into (A.1) and (A.2) and apply the variational method, we have

$$\begin{aligned}
\delta W &= \delta U - \delta V \\
&= D \left[\iint_{\Omega} \nabla^4 w \delta w dx dy + \int_{\partial\Omega} \nabla^2 w \frac{\partial \delta w}{\partial n} ds - \int_{\partial\Omega} \left(\frac{\partial^3 w}{\partial x^3} + \frac{\partial^3 w}{\partial x \partial y^2} \right) \cos \alpha \delta w ds \right. \\
&\quad \left. - \int_{\partial\Omega} \left(\frac{\partial^3 w}{\partial y^3} + \frac{\partial^3 w}{\partial x^2 \partial y} \right) \sin \alpha \delta w ds \right] + D_g \left[\int_{\partial\Omega} \left(\frac{\partial^2 w}{\partial x^2} \sin^2 \alpha - 2 \frac{\partial^2 w}{\partial x \partial y} \sin \alpha \cos \alpha \right. \right. \\
&\quad \left. \left. + \frac{\partial^2 w}{\partial y^2} \cos^2 \alpha \right) \frac{\partial \delta w}{\partial n} ds - \int_{\partial\Omega} \frac{\partial}{\partial s} \left[\left(\frac{\partial^2 w}{\partial x^2} - \frac{\partial^2 w}{\partial y^2} \right) \sin \alpha \cos \alpha + \frac{\partial^2 w}{\partial x \partial y} (\sin^2 \alpha - \cos^2 \alpha) \right] \delta w ds \right] \\
&\quad - \iint_{\Omega} q \delta w dx dy - \iint_{\Omega} N_x^o \frac{\partial^2 w}{\partial x^2} \delta w dx dy - \iint_{\Omega} N_y^o \frac{\partial^2 w}{\partial y^2} \delta w dx dy - 2 \iint_{\Omega} N_{xy}^o \frac{\partial^2 w}{\partial x \partial y} \delta w dx dy \\
&\quad + \int_{\partial\Omega} N_y^o \frac{\partial w}{\partial y} \sin \alpha \delta w ds + \int_{\partial\Omega} N_x^o \frac{\partial w}{\partial x} \cos \alpha \delta w ds + \int_{\partial\Omega} N_{xy}^o \frac{\partial w}{\partial y} \cos \alpha \delta w ds \\
&\quad + \int_{\partial\Omega} N_{xy}^o \frac{\partial w}{\partial x} \sin \alpha \delta w ds + \int_{\partial\Omega} M_n^o \frac{\partial \delta w}{\partial n} ds - \int_{\partial\Omega} \left(Q_n + \frac{\partial M_{ns}}{\partial s} \right) \delta w ds \\
&= 0 \quad (A.14)
\end{aligned}$$

Combine the surface and line integrals in (A.13), respectively, we find

$$\iint_{\Omega} (D\nabla^4 w - q - N_x^o \frac{\partial^2 w}{\partial x^2} - N_y^o \frac{\partial^2 w}{\partial y^2} - 2N_{xy}^o \frac{\partial^2 w}{\partial x \partial y}) \delta w = 0 \quad (\text{A.15})$$

$$\int_{\partial\Omega} [D\nabla^2 w + D_g (\frac{\partial^2 w}{\partial x^2} \sin^2 \alpha - 2 \frac{\partial^2 w}{\partial x \partial y} \sin \alpha \cos \alpha + \frac{\partial^2 w}{\partial y^2} \cos^2 \alpha) + M_n^o] \frac{\partial \delta w}{\partial n} ds = 0 \quad (\text{A.16})$$

$$\int_{\partial\Omega} \left[\begin{aligned} & D \left[\left(\frac{\partial^3 w}{\partial x^3} + \frac{\partial^3 w}{\partial y^2 \partial x} \right) \cos \alpha + \left(\frac{\partial^3 w}{\partial y^3} + \frac{\partial^3 w}{\partial x^2 \partial y} \right) \sin \alpha \right] + D_g \frac{\partial}{\partial s} \left[\left(\frac{\partial^2 w}{\partial x^2} - \right. \right. \\ & \left. \left. \frac{\partial^2 w}{\partial y^2} \right) \sin \alpha \cos \alpha + \frac{\partial^2 w}{\partial x \partial y} (\sin^2 \alpha - \cos^2 \alpha) \right] - N_x^o \frac{\partial w}{\partial x} \cos \alpha - \\ & \left. \left[N_y^o \frac{\partial w}{\partial y} \sin \alpha - N_{xy}^o \frac{\partial w}{\partial x} \sin \alpha - N_{xy}^o \frac{\partial w}{\partial y} \cos \alpha + Q_n^o + \frac{\partial M_{ns}^o}{\partial s} \right] \right] \delta w ds = 0 \quad (\text{A.17}) \end{aligned} \right.$$

Therefore, the governing equation (2.13) is obtained from (A.15), and the boundary conditions (2.16-2.18) are obtained from (A.16) and (A.17).